

In.To. COVID-19 Socio-epidemiological Co-causality

Elroy Galbraith

Hokkaido University

Matteo Convertino (✉ matteo@ist.hokudai.ac.jp)

Tsinghua University <https://orcid.org/0000-0001-7003-7587>

Jie Li

Hokkaido University

Victor Del-Rio Vilas

WHO

Article

Keywords:

Posted Date: June 1st, 2021

DOI: <https://doi.org/10.21203/rs.3.rs-571447/v1>

License:   This work is licensed under a Creative Commons Attribution 4.0 International License.

[Read Full License](#)

Version of Record: A version of this preprint was published at Scientific Reports on April 6th, 2022. See the published version at <https://doi.org/10.1038/s41598-022-09656-1>.

1 **In.To. COVID-19 Socio-epidemiological**
2 **Co-causality**

3 **Elroy Galbraith^a, Matteo Convertino^{a,b*}, Jie Li^a, Victor Del**
4 **Rio-Vilas^c**

5 ^a Nexus Group, Faculty and Graduate School of Information Science and
6 Technology, Hokkaido University, Sapporo, JP

7 ^b Institute of Environment and Ecology, Tsinghua Shenzhen International
8 Graduate School, Tsinghua University, Shenzhen, China

9 ^c SEARO/WHO, New Delhi, India

10 May 26, 2021

11 *Corresponding author:* * M. Convertino, Tsinghua Shenzhen International Graduate
12 School, University Town of Shenzhen, Tsinghua Park, Nanshan District, Shenzhen 518055
13 P.R. China, email: matconv.uni@gmail.com
14

15 *Keywords:* infodemiology, infoveillance, positivity, healthcare pressure, misinformation

Abstract

17 Social media can forecast disease dynamics, but infoveillance remains focused on
18 infection spread, with little consideration of media content reliability and its relationship
19 to behavior-driven epidemiological outcomes. Sentiment-encoded social media indicators
20 have been poorly developed for expressed text to forecast healthcare pressure and infer
21 population risk perception patterns.

22 Here we introduce Infodemic Tomography (InTo) as the first web-based interactive
23 infoveillance cybertechnology that forecasts and visualizes spatio-temporal sentiments
24 and healthcare pressure as a function of social media positivity (i.e., Twitter here), con-
25 sidering both epidemic information and potential misinformation. Information spread is
26 measured on volume and retweets and the Value of Misinformation (VoMi) is introduced
27 as the impact on forecast accuracy where misinformation has the highest dissimilarity
28 in information dynamics. We validate InTo for COVID-19 in New Delhi and three other
29 SE Asian cities. We forecast weekly hospitalization and cases using ARIMA models and
30 interpolate spatial hospitalization using geostatistical kriging on inferred risk percep-
31 tion curves between tweet positivity and epidemiological outcomes. Geospatial tweet
32 positivity tracks accurately $\sim 60\%$ of hospitalizations and forecasts hospitalization risk
33 hotspots along risk aversion gradients. VoMi is higher for risk-prone areas and time
34 periods, where misinformation has the highest predictability, with high incidence and
35 positivity manifesting popularity-seeking social dynamics.

36 Hospitalization gradients, VoMi, effective healthcare pressure and spatial model-data
37 gaps can be used to predict hospitalization fluxes, misinformation, capacity gaps and
38 surveillance uncertainty. Thus, InTo is a participatory instrument to better prepare and
39 respond to public health crises by extracting and combining salient epidemiological and
40 social surveillance at any desired space-time scale.

41 *“Not everything that can be counted counts*
42 *and not everything that counts can be counted”’*
43 Albert Einstein
44

45 **1 Introduction**

46 **1.1 COVID-19 and Infeveillance**

47 The spread and magnitude of COVID-19 is reflected in social media production and senti-
48 ments with the lowest ever recorded trend in population positivity (see the Hedonometer at
49 https://hedonometer.org/timeseries/en_all/). Not only are social media messages the
50 saddest they have been since happiness monitoring began (see [Dodds et al. \(2011\)](#)), but the
51 volume of misinformation has grown exponentially ([Gallotti et al., 2020](#); [Islam et al., 2020](#)).
52 These observations provide evidence of the relevance of socio-technological systems like so-
53 cial media to predict epidemiology. Empirical evidence for many diseases before COVID-19
54 and previous analytical findings made clear the linkage between risk perception and infection
55 patterns ([Maharaj and Kleczkowski, 2012a](#)); thus, highlighting the co-causality of social and
56 epidemiological information beyond their predictability.

57 Aware of these linkages, global response to COVID-19 by health authorities includes risk
58 communication messages, e.g. on increasing social distancing and using masks to reduce inter-
59 person transmission. Similarly, messages on enhancing early identification, isolation and care
60 for patients all in a bid to “flatten the curve” shed light on the importance of surveillance
61 and public health capacities ([Thunström et al., 2020](#)). The search for social surveillance
62 tools that could help public health officials to monitor, forecast, plan, evaluate and prepare
63 for public health demand started well before COVID, e.g. with seasonal influenza in USA
64 coupled to predictive multimodeling (see [Paul et al. \(2014\)](#), [Santillana et al. \(2015\)](#) and
65 [McGowan et al. \(2019\)](#)), due to the recognition of the limitations – e.g. delays, misreporting
66 – of traditional epidemiological surveillance systems. In analogy, social media signals are
67 also used to forecast, a priori or in near real-time, extreme environmental phenomena such
68 as earthquakes ([Sakaki et al., 2010](#)), which highlights the relevance of temporal and spatial
69 social media for surveillance.

70 Concurrently to the spread of COVID-19 epidemic, health authorities are combating an
71 infodemic, strictly defined as the rapid exponential increase in the volume of potentially

72 misleading information about an event (WHO et al., 2020). Misinformation, considered as
73 objectively false or inaccurate information, is of difficult detection and classification because
74 it is highly affected by perception bias. Misinformation can tangibly and negatively impact
75 response strategies and health-seeking behaviors (Ung, 2020; Otto and Eichstaedt, 2018; Ma-
76 haraj and Kleczkowski, 2012b) which may lead to increased infections and hospitalization.
77 Against this background, infodemiology and infoveillance (Eysenbach, 2009) emerge as a
78 strong public health response to the COVID-19 pandemic. Infodemiology applies principles
79 of epidemiology to the study of emergence and spread of misinformation, while infoveillance
80 applies information technology solutions to the monitoring and forecast of disease spread
81 as well as visualization of salient outputs (from main patterns to predictions). Prior to
82 COVID-19, scientists have been able to use internet dynamics and message sentiments to
83 monitor public health related phenomena and forecast disease spread (Ginsberg et al., 2009;
84 Eysenbach, 2009; Bragazzi, 2013; Eichstaedt et al., 2015; Santillana et al., 2015; Radin and
85 Sciascia, 2017). However, no model or information system used social media sentiments to
86 forecast sentiments (as continuous variables versus categorical emotions) and healthcare pres-
87 sure (cases and hospitalization) together, over space and time; epidemiology and information
88 patterns have always been disjoined, yet neglecting the ability to quantify the effective impact
89 of information – and misinformation alike – on populations.

90

91 1.2 Information-Prediction Nexus

92 A different perspective on public health forecasting is brought by proposing an assumption-
93 free minimalist model that is focused on patterns rather than processes of the phenomena
94 considered. The employed information-theoretic models (perfectly fitting the general aims
95 of infoveillance) are using the necessary and sufficient social data as sentinels of change,
96 coupled to epidemiological information, to maximize prediction accuracy for the patterns
97 investigated. Information theoretic models like the one proposed here are the least biased
98 models (mechanisms-free) for capturing which set of information is relevant for predicting
99 patterns. Other underlying causal factors, such as local language and socio-environmental
100 factors of the population considered, are certainly important in the domain of physical reality
101 but not in the information domain of predictions. Therefore, the focus is on predictive
102 causality rather than true causality (Li and Convertino, 2020); a principle that, however,
103 should be associated to any model considering the fundamental reality of any model as a
104 microscope of reality rather than its utopian replica.

105 With the aforementioned reasoning in mind, social and epidemiological processes (and yet
106 data about them) are linked by information and misinformation that is revealing patterns
107 of people behavior in terms of sentiments (informative of risk perception) and cases, respec-
108 tively. Additionally, strong predictive causality in process-related variables has been shown to
109 coincide with physical causality; yet, computation that screens and weights information can
110 be used to infer co-causality between two signals robustly, without imposing any assumption
111 a priori on model structure.

112 In the current COVID-19 context, we are interested in knowing whether modern social
113 media are predictive of explosive epidemics, and more precisely which social chatter features
114 are the most predictive of epidemiological patterns. Moreover, whether social chatter features
115 can be accurately used as early warning predictors of risk before cases occur, and how early
116 can forecasts be made. Motivated by these questions we developed InTo as an exploratory tool
117 to quantify how much perceived risk inferred from social chatter in advance was predictive of
118 actual observed risk in cases and extreme cases (or hospitalization) reported by official public
119 health surveillance. This modus operandi and modern infoveillance tool, beyond assessing
120 how much waves in socio- and health-scapes copredict each other via joint “infoscapes”, can
121 validate classical surveillance systems (which provide data that are byproducts of behavioral
122 models, oftentimes affected by strong bias) considering the temporal gap between model and
123 data for multiple surveillance criteria (Vilas et al., 2017). Theoretically, the smaller the gap
124 over time the higher the surveillance accuracy.

125 **1.3 InTo: Infodemic Tomography**

126 Infodemic Tomography (In.To. or InTo hereafter) was developed as a cybertechnology to
127 forecast one week in advance COVID-19 related cases, hospitalizations, population positiv-
128 ity, misinformation impact and spreading, healthcare satisfaction and space-time surveillance
129 uncertainty by leveraging geospatial Tweets and epidemiological data in New Delhi. InTo
130 analyzes and visualizes “tomograms” or snapshots of epidemiological and information dy-
131 namics for the selected geographies. Thus, InTo is proposed as a Digital Health platform
132 for Participatory, Predictive, Personalized, Preventive and Precise Health (“P5”), that is an
133 “upgrade” with respect to the “P4” purview of health, such as in Alonso et al. (2019), via
134 the *precise* identification and provision of systemic health-related information to individuals
135 and populations alike. Weather forecasting is the general epitome of InTo considering its
136 focus on predicting patterns of healthcare pressure as a function of dynamically updated
137 information; thus the InTo dashboard is ideally like an App visualizing the most updated

138 weather forecasts.

139 Previous efforts have focused on internet-based social media for incidence surveillance and
140 outbreak forecasting (Barros et al., 2020). Some of these efforts incorporated hospital visit
141 data in their models (Ram et al., 2015) but none of them coupled social and epidemiological or
142 healthcare information together. InTo goes beyond temporal incidence predictions because it
143 aims to investigate changes in socio-epi patterns over time and space and the value of spatial
144 social chatter by dynamically calibrating the model as data from social and epidemiological
145 surveillance is updated. In this optic and in relation to the early forecasting nature of InTo,
146 the predicted hospitalization is informative of people potentially in need of hospitalization
147 one week in advance. Gradients of hospitalization over space are indicative of patient hospital
148 loads. In an hydroclimatological analogy, gradients of healthcare pressure are like gradients
149 in atmospheric pressure dictating where ill people/rain will likely flow, and exceedance of
150 pressure over healthcare capacity are like floods.

151 Considering previous efforts, InTo is the first cyberinfrastructure to forecast COVID-19
152 specific healthcare pressure (as difference between point- and city-scale predicted cases and
153 hospitalization) as a function of text positivity where the latter is a variable quantifying
154 potential happiness in words shared via social media, i.e. Twitter in this context. Although
155 InTo is not the first to examine the relationship between Twitter sentiments and diseases,
156 previous efforts were based on extracting few categorical emotions or using volume of social
157 media entries as predictive functions (Haghighi et al., 2017; Rocchetti et al., 2017; Eichstaedt
158 et al., 2015; Wilson et al., 2014b). InTo instead is the first effort, set of models and par-
159 ticipatory dashboard to use quantitative measures of continuous sentiments (associated also
160 to potential misinformation) as positivity to forecast healthcare pressure over space and one
161 week in advance, coupled to the evaluation of those forecasts within an information-theoretic
162 framework.

163 In the development of InTo we chose to call happiness, introduced by Dodds et al. (2011).
164 as positivity because it is semantically a more general word that does not imply happiness
165 (strict sensu) and relates more effectively to risk behavioral patterns (related to the objective
166 relative risk conditional to the geographical area considered), at least conceptually. Gradi-
167 ents in positivity as a function of cases or hospitalizations define risk perception patterns on
168 which predictive models are calibrated to produce forecasts. Linear predictive models are
169 used to perform infection and hospitalization predictions whose predictive power is tested
170 via non-linear predictability indicators (i.e., Transfer Entropy measuring the time delayed
171 uncertainty reduction between positivity and epidemiological variables, as discussed in the

172 Material, Methods and Implementation section). These indicators are based on probability
173 distribution functions of the variables of interest and yet they consider uncertainty distribu-
174 tion attributable to other unexplained uncertainty sources. In this broad framework, properly
175 calibrated positivity fluctuations are good sentinels of relative hospitalization risks – and yet
176 good predictors – as much as heat index fluctuations are good sentinels of extreme temper-
177 ature hospitalization (Liu et al., 2018) to mention an analogous public health effort focused
178 on detecting optimal indicators for risk communication.

179 The paper presents the workflow in Fig. 1 and implementation of InTo by using the case
180 of New Delhi to demonstrate its applicability and utility for COVID-19 and in general for
181 any disease. Part of the demonstration includes results of validation exercises conducted to
182 evaluate the developed models. We then discuss limitations of InTo, especially in terms of
183 data availability, representativeness and model complexity. We conclude by outlining future
184 work for InTo.

185

186 2 Case Study Results

187 Here we present InTo as an infoveillance system for the case of New Delhi during the COVID-
188 19 pandemic between April and July 2020. New Delhi is chosen as the prototypical city to
189 display because of its highly coupled social and epidemiological dynamics as empirically
190 found from data. In InTo, once the user selects their city of interest, results of analyses are
191 displayed as a series of visualizations divided into four main sections corresponding to tabs
192 of the dashboard: Healthcare Pressure, Emotions and Misinformation, Predictability and
193 Tweet Spread (Figs. 2-6).

194 2.1 Healthcare Pressure

195 The layout of the Healthcare Pressure tab is displayed in Figures 2 and 3. In New Delhi be-
196 tween April 15 and July 30 public positivity captured from COVID-19 related tweets ranged
197 between 5.6 and 6.0 with a slight downtrend from 5.85 at the beginning of the period to 5.73
198 at the end. Meanwhile, there was a trend reversal in new cases and the cumulative hospital-
199 ization, with new hospitalizations showing an increase in the magnitude of fluctuations closer
200 to the end of the period. Positivity was at its lowest in June when cumulative hospitalizations
201 was at its highest but positivity was highest in July when hospitalization began to increase

202 again. By using the linear relationship between hospitalization and positivity (see ARIMA
203 model at Eq. 5.3), on July 30th we predicted next week’s hospitalization to decrease by
204 381 hospitalizations (i.e. new hospitalizations displayed in the left plot of the dashboard),
205 and cases to increase by 549. Cumulative hospitalization and cases were about 20,000 and
206 1500 on July 30th (left plots in the dashboard). In Figure 8 we present the results of using
207 positivity from all tweets to forecast daily new hospitalization and daily new cases. Spatial
208 forecasts related to misinformation are not shown spatially. Considering the spatial distribu-
209 tion of positivity and hospitalization in the two weeks before forecasting, via geostatistical
210 kriging (Eqs. 5.4-5.7) we forecasted two large clusters of hospitalization in the North-West
211 and South-East and a smaller cluster in the center of New Delhi. In the high healthcare
212 pressure areas colored in red, we estimated that there would be almost 200 new individuals
213 in need of hospitalization (see color bar in the dashboard screen). These are calculated via
214 the geokriging model (Eqs. 5.4-5.7).

215 In order to highlight spatial gradients of hospitalization (meaningful of potential mobility
216 gradients of people in need of hospitalization mediated by the presence of healthcare facil-
217 ities; see Fig. 3) we decided to visualize healthcare pressure H_{P_i} , that is calculated as the
218 difference between locally expected hospitalization and average hospitalization (Eq. 5.8).
219 The numbers displayed on the top of the dashboard refer to expected new hospitalization
220 and hospitalization change from ARIMA (Eq. 5.3) for the entire city. H_{P_i} is visualized in
221 a green-red color shade (where red is for the highest H_{P_i}) for M randomly generated points
222 (10,000) over the city which are interpolated using the geokriging using the semivariogram
223 of positivity. The area encompassed by each point is in the range 0.5-1.0 km^2 , depending on
224 the spacing between points; thus, our forecasts provide a high spatial resolution compared to
225 surveillance systems. The 200 newly predicted hospitalizations displayed in the dashboard
226 constitute the peaks above the average (or the maximum healthcare pressure) in the entire
227 city. The average is ~ 12 according to the geokriging, and that corresponds to the ARIMA
228 average shown on the top of the dashboard (see Fig 2). The average new hospitalizations
229 matches matches very closely the observed hospitalizations from surveillance (i.e. 11). Note
230 that ~ 200 hospitalizations are for few areas in the city and these extreme values are well
231 above the average value for the period considered. The total number of hospitalization in a
232 selected area can be calculate as sum of new hospitalizations for all the points in that area.

233 Considering these results for the week displayed, hospital managers may wish to focus
234 their attention to the North-West and South-East areas of New Delhi (lacking healthcare ca-
235 pacity as displayed by the geolocated and visualized hospitals in Fig. 2) where individuals in

236 need of hospitalizations are potentially looking for treatment in other areas, and thus estab-
237 lishing hospitalization fluxes. Positivity fluctuates around the same city-specific mean, while
238 cumulative hospitalization grows exponentially over the course of the epidemic. Theoretical
239 Gaussian and exponential variograms were the best fit for positivity and for cumulative hos-
240 pitalization, as expected considering their time dynamics (left plots in the dashboard in Fig.
241 2).

242 Figure 3 shows a snapshot of forecasts in mid July 2020 when very distinct clusters of
243 hospitalizations are identified. The figure serves to highlight how gradients in hospitalization
244 pressure are meaningful of potential mobility of people in need of hospitalization and this
245 expected mobility is dependent on local healthcare capacity that determines the ability to
246 treat patients in need. Effective healthcare pressure can be calculated by considering lo-
247 cal healthcare capacity (as number of beds, ventilators or other resources needed to treat
248 patients) and expected hospitalization.

249 **2.2 Emotions, Top Words, and Misinformation**

250 Emotions, from emotion inference algorithms (see Section 5.3), are extracted from the sys-
251 temic information (all the tweets), misinformation tweets, and healthcare-specific tweets
252 throughout the epidemic. Tweets for each category are reported on the right of the tab
253 (Fig. 4) and some of these tweets can be directly reported to InTo as misinformation by so-
254 cial media (Twitter) users. Below we report results that can be inferred by using InTo, such
255 as specific events, word pairs, users and associated emotions. When considering all tweets,
256 the dominant emotion over time was trust, followed by fear and anticipation; joy and sadness
257 were the next most frequent; surprise and disgust were expressed the least. This distribution
258 was observed for the subset of tweets related to misinformation as well, however there was
259 one day, on June 10th, when these tweets expressed more fear than they did trust. As for
260 tweets related to healthcare, trust was usually most expressed, but it was not as dominant
261 as in the case of all tweets or misinformation. Furthermore, sadness seemed to be expressed
262 much more among these tweets, especially in early June. On June 10, the saddest day con-
263 sidering healthcare tweets, the most retweeted tweet was from a user who felt abandoned
264 and helpless after struggling to help his sister and her two small children after her husband
265 had died from the disease. Similar tragic tweets reported the lowest positivity. The most
266 frequent healthcare tweets were also about the lack of beds, inability of hospitals to provide
267 proper service, and the possibility of public health officials to hide the true number of cases.
268 Worryingly, users were also taking the opportunity to request blood donors via Twitter. On

269 July 22nd 2020, the most frequent pairs of words referenced were about “public health ad-
270 vice” and “self-quarantine at home”. A review of the raw tweets showed that many of the
271 tweets were actually tweets of news articles made by organizations rather than individuals.
272 Such tweets tended to be “neutral” in their positivity (i.e. centered around 5 without an
273 increasing or decreasing trend), with values ranging between 4 and 6. This emphasizes the
274 tendency of organizations, versus individuals, in manifesting risk-neutral perception patterns
275 corresponding to average values of positivity.

276 **2.3 Predictability and Forecasting**

277 Predictability indices (Section 5.5) are reported in Figure 5 for both cases and hospitalizations
278 as values over 100; yet, percentage changes are easily quantifiable. The risk index confirmed
279 that cases were declining over time, despite momentary increases. This index showed the
280 same trend for the full tweet and misinformation datasets because it is based on the same
281 data (the time series are reported twice to compare infection and hospitalization trends
282 against systemic information and misinformation indices). A model-based risk indicator can
283 be calculated to visualize the risk in terms of predicted values rather than data only.

284 Between May and June tweet positivity was under-predicting cases but then began to
285 over-predict cases in July. Tweet positivity and cases showed a mostly moderately negative
286 correlation (mean corr= -0.24). Although the value of the correlation was constant, suggesting
287 a reliable model or stable dynamics, predictability was not stable until late June, when the
288 predictability indicator became very small indicating lack of non-linearity, and thus implying
289 high reliability in the linear forecasting of cases via the ARIMA model. All results suggest
290 that tweet positivity from all downloaded tweets was most meaningful for forecasting the
291 spatio-temporal spread in July, with relatively high uncertainty earlier. July has the highest
292 correlation coefficient (in magnitude), lowest gap and non-linear predictability, as well as the
293 lowest VoMi (Eq. 5.13). The subset of tweets related to misinformation showed a similarly
294 negative though much weaker correlation with cases (mean corr = -0.01). This is concordant
295 to the much higher non-linear predictability of misinformation manifesting the decreasing
296 forecasting accuracy of ARIMA for this tweet subset.

297 When considering all tweets, the model mostly under-predicted hospitalizations, with its
298 largest under-prediction occurring in late June after hospitalization became the largest in
299 the end of May (bottom left plot of Fig. 5). The largest over-prediction was observed in
300 late July after hospitalization risk became very large. Yet, very large spikes in risk seemed

301 to produce very large gaps in predictions. These large gaps are driven by misinformation
302 as shown by the VoMi assessment that is higher at the end of the monitored period. The
303 value of misinformation (Eq. 5.13) showed a gradual uptrend, indicating that tweets related
304 to misinformation were decreasing the forecasting accuracy (based on linear correlation) of
305 all tweets for cases and hospitalization as time progressed. Tweet positivity was mostly
306 negatively correlated with hospitalization but predictability was low, especially for hospital-
307 ization. This underlines the fact that there is more linearity between new hospitalization and
308 positivity than cases and positivity, and yet the ARIMA forecasts are more reliable for new
309 hospitalization. Despite this average result we observe that larger fluctuations in indicators
310 are seen for hospitalization than cases, likely underlying the necessity to include other pre-
311 dictors for extreme hospitalization events. Lastly, time series of indicators for all tweets and
312 misinformative tweets are quite similar due to the low detection of misinformation; nonethe-
313 less time-point values are different as manifested by VoMi because misinformation, although
314 small, exist and impact forecasts.

315 **2.4 Tweet Spread**

316 The Tweet Spread tab (Fig. 6) shows the volume of tweets and retweets, as well as their
317 positivity, for the systemic information and misinformation set. There were between 10,000
318 and 100,000 tweets per week related to COVID-19 in New Delhi. The volume of retweets was
319 much lower in comparison, not exceeding 10 retweets, and had positivity values approach
320 6 meaning they were more positive than the average neutral value of 5. Additionally, both
321 tweet volume, retweets and positivity are slowly decreasing over time which manifest the
322 lower COVID information production and decreasing positivity.

323 The number of misinformation tweets was the highest in the early days of the pandemic
324 descending relatively rapidly as time progressed. The retweet volume was very low com-
325 pared to the full tweet set (the difference is about three orders of magnitude) and most of
326 the popular misinformative tweets had low positivity. One of these popular misinformation
327 tweets called for the protection of citizens of different religions who were being implicated
328 and arrested on false charges. This tweet underlines the fact that misinformation is not nec-
329 essarily carrying deceiving information but also information about perceived wrong behavior
330 in populations. Thus, misinformation can capture more the dichotomy between common and
331 divergent groups in the area analyzed. The large difference in volume of all tweets ($\sim 10^5$) and
332 misinformative tweets (that are less than 10^3 , two orders of magnitude less than all Tweets)
333 explains why time series dynamics of predictability indicators for the systemic information

334 and misinformation predictors (Fig. 5) is very similar but time point values are different.

335

336 2.5 Model Calibration and Validation

337 Results of the model validation over space (for the optimal predictor set) are displayed in
338 Figure 7. Plot A shows the forecast of spatial hospitalization based on geospatial tweet
339 positivity and city scale hospitalization. Predicted hospitalization based on Tweet positivity
340 suggested there would be high hospitalization pressure H_P (Eq. 5.8) in areas, such as Narella,
341 Gurugram and Dwarka (SW part of the city), which were unaccounted for by the monitoring
342 system just focused on bed occupancy (and yet on models based on that occupancy shown
343 in plot C and D). The highest peak of H_P is 160 and the average of healthcare pressure
344 over space is very close to the average of hospitalization at the city scale. However, the
345 geographical distribution of healthcare pressure is different from the distribution of hospi-
346 tals because geokriging is extending spatially the positivity-hospitalization relationship (that
347 shows an inverse proportionality between these variables) that is beyond hospital locations.
348 Nonetheless, tweet locations highly predict hospital locations as binary variables (Fig. 7B).

349 When performing interpolation via geokriging based on hospital-scale data alone (Fig.
350 7D), high hospitalization was predicted in the center of the city, with gradients of hospital-
351 ization decreasing outwards. This predicted hospitalization reflects ($\sim 80\%$) the distribution
352 of bed occupancy as expected. The predicted hospitalization considering hospital-scale occu-
353 pancy and positivity (Fig. 7C) matches 85% the hospitalization based on hospital data only
354 (Fig. 7D). The former is however predicting higher hospitalization in other areas beyond
355 hospital areas, and this emphasizes the fact that the model is also predicting healthcare pres-
356 sure as individuals likely in need of hospitalization. Note that the range of hospitalization for
357 predictions of plots C and D in Fig. 7 are the same with maximum cumulative hospitalization
358 equal to ~ 65 for the period 21 July-11 August 2020.

359 Figure 8 shows the calibration and validation of the ARIMA model which is useful for
360 selecting the optimal set of predictors. The results of ARIMA forecasts with different models
361 in terms of predictors are shown for cases, cumulative and new hospitalizations for New
362 Delhi. ACF is ARIMA based on epidemiological data only, while all other ARIMA models
363 are based on positivity, Tweet volume, Tweet volume and positivity combined. The model
364 that minimizes the mean absolute percentage error (MAPE, in insets) is based on positivity
365 only because of its highest predictive power for fluctuations in healthcare pressure (cases and

366 hospitalization). However, the model with volume and positivity has similar MAPE because
367 of the ability of volume to predict the largest extreme variations in hospitalization. MAPE is
368 larger for new hospitalization than cumulative hospitalizations due to the larger stochasticity
369 of the former than the latter over time. The departure of forecasted values from observations
370 is the gap index in the dashboard (Fig. 5).

371 The (p, d, q) parameters of the ARIMA model (Section 5.4.1) manifesting seasonality,
372 memory and fluctuations are on average $[0, 1, 1]$ for all models including ACF, $[0, 1, 2]$ toward
373 the end of the monitored period that highlights the increase importance of fluctuations,
374 and $[1, 1, 2]$ for volume and positivity that highlights the higher seasonality of tweet volume
375 and ability to capture larger extremes. (p, d, q) parameters increase if misinformation is
376 used when predicting hospitalization and cases, and this is in synchrony with our findings
377 that non-linear predictability increases because of the higher memory long-range effects of
378 misinformation. Average results of social and epidemiological variables for New Delhi are in
379 Table 1 considering different areas of the city and time periods.

380 **3 Discussion**

381 We have demonstrated the use of InTo to calculate tweet positivity to forecast and predict
382 the spatio-temporal spread of COVID-19 healthcare pressure. However, the model can be
383 applied to any disease or public health phenomena of interest via properly tuning the fore-
384 casting models. In New Delhi we inferred that the population was relatively positive in the
385 messaging, expressing mostly trust, despite the high case load and hospitalization. This weak
386 negative correlation manifesting risk aversion – due to the expected decrease in positivity for
387 increases in hospitalization – was statistically useful for predictability purposes considering
388 both geostatistical kriging and ARIMA models that use correlation values (Eq. 5.3. and 5.7).

389 We showed that hospitalizations could be expected to concentrate in certain areas of the
390 city, suggesting those clusters to be the focus of additional public health surveillance and
391 healthcare resources since new hospitalizations may occur. We found that misinformation
392 does affect the accuracy of the model and provides another illustration of the impact of
393 misinformation: it can impact even our ability to properly forecast healthcare pressure but
394 not necessarily negatively (in terms of reduction of prediction accuracy) throughout the
395 pandemic. This impact was found to be positive, yet improving prediction accuracy, at the
396 beginning of the epidemic (despite the higher volume of misinformation) and negative at the
397 end of the epidemic likely because the delayed effect of misinformation spreading.

398 **3.1 Data Uncertainty**

399 The success of any intelligence tools rests also on the availability of data. Better quality data
400 can likely support more accurate and more meaningful forecasts. Better data refers not only
401 to the representativeness of the data but also to the granularity and compatibility of the data
402 as well in relation to what is predicted. In terms of granularity, this could be hospital level
403 rather than state or national level hospitalization data for example. We showed in Fig. 7 that
404 the geostatistical kriging model performs much better – in terms of predicted hospitalization
405 – when spatially explicit hospital data are provided, particularly when the objective is also
406 to capture reported bed occupancy rather than average expected hospitalization at the city
407 scale solely. Compatibility would mean not only using universally accepted terminology, but
408 formatting the data in the same way to ease data processing. Certainly a huge discrepancy
409 exist between social and epidemiological data (considering spatial and temporal resolutions as
410 well as data volume), and then data processing becomes a time consuming process potentially
411 carrying systematic uncertainties. Technology exists to translate data which is formatted
412 differently, but it remains important that data stewards communicate with epidemiologists,
413 “infodemiologists” and decision makers to determine a usable design. This is particularly
414 important in the context of pandemics and emerging infectious diseases although localized.

415 Our concern is directed more towards epidemiological data rather than social media data.
416 Social media users generate terabytes of data and many platforms have policies that allow
417 restricted access to data, especially for academic purposes or some other public good purpose.
418 However, epidemiological data has proven to be more difficult to collect and share. This would
419 take effective coordination as hospital managers and public health officials collate and share
420 data via application programming interfaces (API) for highest efficiency and timeliness in
421 generating results.

422 **3.2 Population Representativeness of Data**

423 An issue connected with data availability is the matter of representation, that is, the extent
424 to which the data include enough heterogeneity to reflect the complexity of the population
425 for which the data set is assembled. This is particularly relevant to social media data such
426 as Twitter data. The demographics of users can differ significantly by biology, socio-cultural
427 and economic class, location and the availability of technological infrastructure (Silver et al.,
428 2019; Sadah et al., 2015; Vashistha et al., 2015; Duggan and Brenner, 2013) so individ-
429 ual/community experiences and perspectives can differ from the wider population (Mellon

430 and Prosser, 2017). Even the choice of language might limit the representativeness of data
431 used in the model: InTo currently uses English, which is spoken in India, but not by a ma-
432 jority. One also has to consider the inclusivity of the search term. Our use of 'OR' instead of
433 'AND' made our search more inclusive rather than restrictive thereby increasing the potential
434 volume of tweets returned. Other choices would have certainly provided other predictability
435 indices; and then one of the future improvements would be extracting the set of constraining
436 hashtags that maximize predictions overall among all possible choices of hashtags. However,
437 this choice would require a much higher computational cost and, in addition, fitting data the
438 closest (versus providing the full range of feasible predictions in a Maximum Entropy perspec-
439 tive) is not always the optimal choice due to the presence of systematic uncertainty in data.
440 Therefore, our current InTo version is not necessarily bounding the model-data gap consid-
441 ering all feasible factors (from language to hashtags), nor a fully causal investigation, but a
442 model defining the simplest and most informative inputs and outputs to represent dynam-
443 ics of population patterns. Further work will define more clearly importance of underlying
444 factors and the absolutely optimal model form.

445 Tweets in a city contain information of spatially separated events about the same process;
446 thus spatial spread of COVID and top tweeted pairs can be calculated over geolocated Tweets.
447 Posting time and content (related to volume and positivity) is very weakly dependent on the
448 social media platform. Additionally, social media users tend to interact outside of their usual
449 social networks or real-world socio-economic class much more on these platforms (Silver et al.,
450 2019), creating opportunities for groups absent from these platforms to be heard in a latent
451 way. Furthermore, tweets report information that may not be reported by official media
452 and/or that may circulate in real life events (e.g. just spoken information). This is also the
453 reason for which InTo can be used by users as a reporting information/misinformation tool
454 via registering their Twitter account. We suggest this "Digital Health" feature particularly
455 relevant for healthcare workers.

456 Twitter penetration can differ between and within countries, but tweets still show high
457 relevance for predicting spatio-temporal patterns of infections and hospitalization. Addition-
458 ally, emotional affects are highly linked to local non-Twitter media and languages, as we see
459 high volumetric correlation with local newspapers articles and retweets of English tweets in
460 local languages. Certainly, demographic and other features of the tweeting population are
461 relevant for how the virus spread but not the whole complexity is needed for forecasting
462 purposes in the short and long term. Nonetheless, this version of InTo is a proof of con-
463 cept version and will likely investigate and include other social media platforms, languages,

464 information features, visualization options, diseases and socio-environmental phenomena in
465 future versions for investigating processes and practical applications.

466 **3.3 Predictive Causality and Forecasting**

467 Even when considering the issues of data availability and representativeness, the advantage of
468 InTo is that it focuses on patterns rather than causation. InTo does not purport to have found
469 nor to be exploiting a causal relationship between tweet positivity and healthcare pressure.
470 Rather, it exploits spatio-temporal patterns and correlations that might not be physically
471 significant (although arguable in an information dynamic sense), but that are nonetheless
472 practically useful probabilistically. The relationship between sentiments and behaviors are
473 quite complex, and there are many other variables in the complex reality of phenomena
474 considered that are however not all needed when forecasting population outcomes. There
475 are population factors such as sex, socio-economic status, proximity to affordable healthcare
476 facilities and the availability of insurance or some other means of paying that certainly impact
477 real processes of individuals. There may even be socio-political realities at play that force
478 individual behavior. However, the key goal of InTo – in a complex system science purview
479 – is the prediction of population patterns considering the most essential predictors without
480 making any assumption on the underlying processes. Complicating the model comes at a
481 cost, not just in the acquisition of data – because such data may not be available or costly to
482 acquire – but also in the applicability of the resultant model that would be highly sensitive,
483 extremely hard to calibrate and full of unchartable uncertainties. A model that enables
484 reliable forecasts with a reasonable level of accuracy given a variety of scenarios should be
485 the ultimate aim of any information system model.

486 In InTo a forecast refers to the estimation of future outcomes (in short term) which
487 uses data from previous outcomes, combined with recent or future trends. Forecasts like
488 those from the application of ARIMA models imply time series and future point estimates,
489 while predictions do not. A prediction is based on probabilistic patterns (e.g. probability
490 distributions, trends, and total uncertainty reductions) and yet of “possible outcomes” in
491 the long-term. This is the case of geokriging and the pattern that can be obtained by using
492 the predictability indicator (Eq. 5.12). Forecasting does not imply predictability nor the
493 contrary, but in principle, optimized forecasting implies strong predictability for the whole
494 time period considered. Vice versa, predictability of patterns does not guarantee the ability to
495 have highly accurate time point estimates. InTo is providing both in order to support public
496 health in almost real-time decision making and long term sensitivity of social surveillance for

497 epidemiological outcomes.

498 **3.4 Value of Misinformation**

499 Identifying misinformation is a chief concern in infodemiology via infoveillance, not to mention
500 in other areas of society like sociology and politics. Methods that use the probabilistic and
501 lexical features of text in order to determine whether they represent misinformation (Li et al.,
502 2019) abound. These methods depend on datasets that contain messages which have already
503 been labelled misinformation by experts a priori. The set of misinforming messages considered
504 by inTo includes tweets already directly labelled as or questioned to be misinformation by
505 users, having most likely already gone through a vetting process. The advantage of this
506 approach is the use of a human- and crowd-based classification which overcomes the challenges
507 of assumption-driven lexical analysis by model. Interestingly, a posteriori we confirmed (via
508 reviewing Tweets one by one and considering their incorrect or false information) that the vast
509 majority ($\sim 95\%$) of misinformative tweets are truly misinformation and this misinformation
510 set showed much larger dissimilarity – in terms of word diversity, volume divergence and
511 asynchronicity – with respect to cases and hospitalization than the full tweet set. This
512 emphasizes how dynamical properties of information are essential in categorizing different
513 types of information, as well as how crowd-based self-reporting is relevant. In the literature
514 there are still some debates about this topic but those seem platform dependent. For example,
515 Jiang and Wilson (2018) suggested that user comments do not provide sufficient predictive
516 power when attempting to classify misinformation, but a recent study (see Serrano et al.
517 (2020)) successfully utilized user comments on YouTube videos instead of parsing these videos
518 to classify misinformation with high accuracy.

519 Our results found that misinformation-related tweets provided at times more time-point
520 accurate forecasts of healthcare pressure than forecasts based on all tweets. We observe
521 that misinformation positivity shifts the forecast error based on all tweets to higher positive
522 values (implying positive VoMi); yet, misinformation is slightly contributing to overprediction
523 but considering its magnitude this overprediction is positive in consideration of surveillance
524 underreporting and other systematic errors. This is not to say that misinformation is good
525 in an absolute sense; in fact, it remains important that accurate facts are disseminated to
526 people as the consequence of acting on incorrect information could imply wrong behavior
527 leading to higher cases and hospitalization. Rather these findings show that misinformation
528 – in its positivity rather than volume or messages – is useful for forecasting. This is related
529 to the use of positivity as a novel aspect in characterizing social media content and to the

530 fact that positivity fluctuations of quickly generated misinformation tend to have long-term
531 consequences on the predictability of the unfolding epidemic (misinformation that of course
532 can have impact on the social behavior of populations). This is manifested for instance
533 by a higher predictability indicator of misinformation (Fig. 5) as well as the higher (p, d, q)
534 parameters of the ARIMA model (Section 5.4.1). Additionally, the full tweet information may
535 contain too much “entropy” of messages that do not quite reflect people sentiments about
536 the epidemic despite not being misinformation. Thus, public health organization could use
537 positivity embedded in misinformation to protect the public, and then seek to eradicate.

538 3.5 Social Value of InTo

539 The most immediate value to society of InTo is through appropriate social media signal
540 monitoring and by complementing traditional epidemiological surveillance which allows opti-
541 mal healthcare planning during public health crises. As a novel and innovative infoveillance
542 cyberinfrastructure (because available online and systematized in its function), apart from
543 monitoring the spread of social chatter, InTo enables the public health system to properly
544 plan for inevitable fluxes of people in need of care.

545 Public health officials and healthcare institutions need a way to cost-effectively determine
546 whether they are able to meet the impending healthcare demands via considering both in-
547 formation and disease epidemics that we showed to be non-trivially and strongly coupled.
548 Additionally, InTo enables public health officials to evaluate customer satisfaction of the
549 healthcare system during the epidemic/pandemic. This is performed by evaluating senti-
550 ments of words related to healthcare in terms of emotions, positivity and specific content of
551 social chatter. Content that can point out specific hospitals, physicians and treatments, as
552 well as users. Thus, individuals are able to review what the general public posts as problems
553 on social media about the local healthcare infrastructure and global issues. Also, information
554 about which institutions are operating beyond their capacity, and what particular depart-
555 ment may be operating poorly or successfully is available. Yet, InTo responds the need
556 of predictive, personalized and precise health in an unprecedented way by both capturing
557 information-driven salient population patterns and individual needs.

558 By monitoring public expressions, InTo provides some insights into emotional affects of
559 the population in response to disease spread. This can also illuminate the importance of
560 psychological states in response to these crises, which may be precursors to post traumatic
561 stress disorders (PTSD). Other studies (Mowery et al., 2017; Wilson et al., 2014a) showed

562 how word choices reflect mental health states in long term and these may be predicted by
563 performing a systemic functional network analysis of the tweet text extracted by InTo. This
564 would also further link latent social and epidemiological outcomes explicitly.

565 Finally, InTo enables to monitor the spread of misinformation during public health and
566 social crises, as well as evaluate the impact of any intervention, in the form of risk communi-
567 cation, they enact. InTo provides volumetric measures of misinformation generation on social
568 media over time and geographical domain, as well as quantifies how misinformation affects
569 forecasts of case and hospitalization (i.e. VoMI) that potentially relate to real-world misbe-
570 havior dependent on circulating misinformation. Therefore, the performance of interventions
571 against misinformation can be measured by the volume of misinformation that is reduced
572 as well as by the uncertainty reduction in forecasts. In this sense, InTo provides an extra
573 evaluation of the surveillance system by considering misinformation as extra uncertainty or
574 uncertainty reduction, depending on its negative or positive impact, on prediction accuracy.
575 Comparison of multiple information sources and model predictions across multiple criteria
576 over time time, is a rigorous and efficient way to evaluate surveillance systems and likely
577 detect the most reliable source of data (Vilas et al., 2017).

578

579 4 Conclusions

580 Infodemic Tomography (InTo) is proposed as a cybertechnology to monitor and visualize
581 the spatio-temporal co-causal variability of social media positivity and healthcare pressure
582 (as cases, hospitalization and misinformation separately) during epidemics and public health
583 crises. The most salient points to mention about InTo are listed below.

- 584 • A clear linkage between epidemiological and information dynamics (in terms of posi-
585 tivity) is detected via linear and non-linear patterns that are potentially revealing risk
586 perception or information availability in populations. These patterns are useful for pre-
587 dictions of epidemic dynamics, complementing traditional surveillance, and analyses
588 of social media dynamics (generation, absorption, spreading, diversity and positivity)
589 that have the potential to design risk communication strategies which aim to enhance
590 or correct information shared in the target populations.
- 591 • Location of tweets is deemed relevant to predict hospitalization where it is officially re-
592 ported (interestingly, ~60% of predictions of hospitalizations coincide with the reported

593 total bed occupancy in the test city of New Delhi and in locations where people are
594 potentially in need of hospitalization. Yet, geospatial tweets (and associated positivity)
595 are convenient transfer functions of epidemiological information to small space-time
596 scales and inform about potential fluxes of healthcare demand that are useful for dy-
597 namic healthcare management. Forecasts of cases and hospitalization are provided at
598 very high resolution ($\sim m^2$) one week in advance by using a linearized ARIMA model.
599 Risk and gap indicators are provided to measure the trend and model-gap difference
600 of the epidemic weekly. A predictability indicator (normalized transfer entropy) is de-
601 veloped to monitor the uncertainty reduction of Twitter positivity for epidemiological
602 dynamics, thus to test the predictive causality versus the forecasting of the ARIMA
603 model.

604 • Misinformation is extracted by directly mining population-reported misinformation (via
605 misinformation-related hashtags) and can be tested a posteriori via manual classifica-
606 tion with public health officers cooperation and automated model-driven testing of
607 dissimilarity (divergence, asynchronicity and diversity) from the systemic COVID-19
608 information over time. The Value of Misinformation (VoMi) is introduced as the im-
609 pact on forecast accuracy calculated as the difference of gap indices (potentially negative
610 over time) for the systemic and misinformation datasets. VoMi trends are city-specific
611 and negative if they are increasing over time because they imply high impact of mis-
612 information on short-term forecasting. VoMi is typically low or negative because it
613 is highly non-linear and yet, not very informative of forecasting sudden events, but it
614 carries higher predictability (as uncertainty reduction) for delayed long-term extremes
615 and probabilistic patterns.

616 InTo encapsulates the future of public health management with the the fusion of multiple
617 surveillance streams: from traditional epidemiological and healthcare data to model-inferred
618 social sentiment data. As technology develops and the public creates and consumes informa-
619 tion via internet, epidemiology will need to consider the spread of social information not only
620 as a problematic element but as a solution for disease tracking and optimal risk communica-
621 tion. For instance, ad-hoc social messages by authorities can counteract misinformation that
622 is sensed online, as well as social media inferred cases (or model predicted) can complement
623 traditional public health surveillance. InTo shows that sentiments from digital messages can
624 forecast the incidence and spread of healthcare pressure for areas besieged by a public health
625 crisis. In terms of forecast, it is near-real time, accurate, reasonably inexpensive and easy to
626 use in a computational sense. Infoveillance tools like InTo can only get better with higher

627 quality data from traditional surveillance systems on which validation should be performed,
628 but more importantly with the collaboration between developers and stakeholders to effec-
629 tively create solutions that are useful for effective decision and policy making. Future work
630 will potentially entail expanding social media platforms and diseases to be monitored. Other
631 validation experiments to improve InTo accuracy and utility are needed in data-rich areas.
632 Via collaborations with public health officers, stakeholders and volunteers with interests in
633 social computing we will seek for releasing InTo as a globally implemented cyberinfrastructure
634 for public health research and practice.

635 5 Material, Methods and Implementation

636 5.1 Twitter Data Mining and Preprocessing

637 Data collection occurred weekly beginning in April 2020. Only English language tweets
638 within a geographical bounding box (reflecting the target geographical area of the cities) were
639 retrieved from Twitter using the `rtweet` package (Kearney, 2019). The choice of English was
640 dictated by the lack of robust computational tools usable for other language translations
641 (also considering the big-data size of tweets) and the complexity of the languages for the
642 country considered (i.e., Hindi, Marathi, Thai, and Indonesian); the latter would make the
643 uncertainty in positivity scoring of words very high.

644 Search terms are hashtags that were identified given their rank on a list of the most pop-
645 ular Twitter terms on a daily and weekly scale (the search was done by comparing <https://getdaytrends.com/> and <https://trends24.in/>). Our search query for the COVID *sys-*
646 *temic information* was constrained to the hashtags “covid OR coronavirus OR quarantine OR
647 stay home OR hospital OR covid OR covid19 OR covid-19 OR coronavirus OR quarantine
648 OR stayhome OR hospital”. Thus, we downloaded close to 30,000 tweets daily between April
649 15 and July 30, 2020 for New Delhi (defined as “National Capital Territory of Delhi” by Twit-
650 ter in the box $28^{\circ}41'25.9''N, 76^{\circ}83'80.7''E$ to $28^{\circ}88'13.4''N, 77^{\circ}34'84.6''E$). We identified the
651 *misinformation* dataset by extracting a subset of our downloaded tweets that contained the
652 terms “misinformation”, “false”, “fake” or “lie”, directly reported by people in their tweets.
653 These were tweets in which a user either identified information or other messages as mis-
654 information or questioned whether that message or information was misinformation. We
655 also identified tweets related to *healthcare* information by extracting those tweets contain-
656 ing the key terms “hospital” or “test”. To preprocess these data we removed punctuation
657 marks and uniform resource locators (urls) using the `tidytext` package (Silge and Robin-
658 son, 2016), and we replaced abbreviations, symbols, contractions, ordinals and numbers with
659 the words they represent using the `qdap` package (Rinker, 2020). `tidytext` was also used
660 to unnest the unigrams (single words) and bigrams (sequential word pairs) from each tweet.
661 Lastly, word stemming was conducted using the `wordStem` function of the `SnowballC` package
662 (<https://cran.r-project.org/web/packages/SnowballC/SnowballC.pdf>) for being able
663 to score affine words in terms of positivity rather than disregarding these words.
664

665 5.2 Epidemiological Data Mining and Preprocessing

666 At the time of our study, epidemiological data was not available for New Delhi specifically
667 (i.e. the case study shown in this paper) nor for local hospitals within the analyzed domain,
668 but rather for the state of Delhi, i.e. the National Capital Region (NCR). The dataset (kp,
669 2020) contained both crowd-sourced and official data from the Ministry of Health and Family
670 Welfare. It included the number of cases and cured, discharged or migrated individuals in
671 the state since March 15, 2020 when India registered its first case. For these motivations
672 we calculated the new daily cases $\Delta I = I(t) - I(t - 1)$ where I stands for cases, and new
673 hospitalization as $\Delta H = H(t) - H(t - 1)$ where hospitalization $H(t) = I(t) - R(t)$ are
674 cases minus the number of patients cured, discharged or migrated. Later we located hospital
675 level data from information reported by the New Delhi from the Ministry of Health and
676 Family Welfare (<https://coronabeds.jantasamvad.org>) which indicated the daily number
677 of hospital beds occupied within a geo-located area. The vast majority of these hospitals
678 resulted to be private hospitals. We conducted validation of our spatio-temporal forecasting
679 model by comparing city-scale calculated hospitalization versus hospital-scale data for the
680 same city. As for Mumbai, the situation was analogous to New Delhi; data of cases and
681 hospitalization was only available at the state scale, i.e. Maharashtra. Thus, cases and
682 hospitalization of Mumbai was calculated as $\sim 50\%$ of the whole state as evidence supported.
683 For Bangkok the same calculation was performed where original data are from [https://www.](https://www.worldometers.info/coronavirus/country/thailand/)
684 [worldometers.info/coronavirus/country/thailand/](https://www.worldometers.info/coronavirus/country/thailand/). Cases are 50% of national cases
685 and hospitalization are 50% of active cases that are used by Thailand as the measure for
686 hospitalization. Active cases in Thailand are defined as total cases minus total deaths and
687 recovered patients, and “represents an important metric for Public Health and Emergency
688 response authorities when assessing hospitalization needs versus capacity” (quoted by the
689 Thailand Ministry of Health). Jakarta was the only city in our InTo application that provided
690 city scale data of cases and hospitalization as independent variables. Data for Jakarta is from
691 the Jakarta Health Department data reported to the Ministry of Health of Indonesia and
692 displayed in <https://corona.jakarta.go.id/en/data-pemantauan>. For daily cases, data
693 displayed in the time series labeled National Jakarta Trend are used. For hospitalization, data
694 displayed in the time series “PDP Data Accumulation Table and Cases Data Accumulation
695 Table” are used. We considered the sum of the reported number of patients currently in
696 hospitals (PDP Data Accumulation Table) and the reported number of patients in intensive
697 care (Cases Data Accumulation Table) as the cumulative hospitalization.

698 5.3 Sentiment Quantification

699 Sentiment analyses performed for InTo involved quantifying both categorical emotions and
700 positivity of each text corpus given unigrams (words) within extracted tweets. The `labMT`
701 lexicon (Dodds et al., 2011), accessed via the `qdap` package, was used to measure the positivity
702 and the `nrc` lexicon (Mohammad and Turney, 2010), accessed via the `tidytext` package, was
703 used to evaluate emotional affects (or categories) in a tweet. The continuous (real number)
704 positivity of a tweet (P) was quantified as:

$$P = \sum_{i=1}^N p_{avg}(w_i) \cdot \frac{f_i}{\sum_{j=1}^N f_j} \quad (5.1)$$

705 where $p_{avg}(w_i)$ is the positivity value of each word (w_i) as indicated in the `labMT` lexicon,
706 and f_i is the frequency of each word. The daily positivity (\bar{P}_t), given N_t number of tweets
707 on day t is calculated by

$$\bar{P}_t = \frac{\sum_{j=1}^{N_t} P_j}{N_t} \quad (5.2)$$

708 where j is indicating all tweets in the day considered. The emotion of a tweet was con-
709 sidered to be the distribution of the affect categories (for example, anger, surprise, joy, etc.)
710 associated with each word of a tweet. We noted the affect categories associated with each
711 unigram and then counted the number of times each affect category appeared in a tweet and
712 in a day. Weekly calculations of positivity and emotion categories are calculated considering
713 average value of sentiments at the weekly scale.

714

715 5.4 Forecasting

716 5.4.1 ARIMA temporal forecasting

717 InTo perform weekly temporal forecasts of new cases and hospitalizations as a function of
718 tweet positivity and historical epidemiological events. A two-step non-seasonal $ARIMA(p, d, q)$
719 model is used for temporal forecasting where parameters p , d , and q are non-negative integers;
720 p is the order (number of time lags) of the autoregressive model considering long term trends
721 (e.g. seasonality), d is the degree of differencing (the number of times data are subtracted to
722 past values) that considers memory for non-seasonal events, and q is the order of the moving-

723 average model for errors establishing their temporal impact. Because (p, d, q) parameters and
724 coefficients are updated weekly in order to optimize forecasts, the model can be considered
725 non-linear despite its linear formulation. Temporal forecasts were calculated using a non-
726 seasonal ARIMA model as implemented in the **fable** package (O’Hara-Wild et al., 2020).
727 The two-step forecast is done because first positivity is forecasted for the week following the
728 one considered and after cases and hospitalization are forecasted based on future positivity.
729 The analytic form of the ARIMA model is written for $y = \Delta H$ as new hospitalization that
730 is the primary target of InTo; however, y can generally be positivity or cases based on the
731 selected predictand. Thus, hospitalization is forecasted as:

$$\Delta H_t^d = \beta_0 + \beta_1 \bar{P}_t + \phi_1 \Delta H_{t-1}^d + \dots + \phi_p \Delta H_{t-p}^d + \theta_1 \varepsilon_{t-1} + \dots + \theta_q \varepsilon_{t-q} + \varepsilon_t \quad (5.3)$$

732 where ΔH is differenced to an order of d (not that d is an index and not a power exponent),
733 β_0 is a constant, β_1 is the regression coefficient for average positivity \bar{P}_t , $\phi_1 y_{t-1}^d + \dots + \phi_p y_{t-p}^d$
734 is an autoregressive model of order p and $\theta_1 \varepsilon_{t-1} + \dots + \theta_q \varepsilon_{t-q} + \varepsilon_t$ is a moving average model of
735 order q . The error terms ε_t of ΔH are assumed to be independent and identically distributed
736 sampled from a normal distribution with zero mean. Thus, ε_t is a white noise factor.

737 Default settings of the ARIMA function in the **fable** package was selected as it automat-
738 ically determines the values of p , d and q that minimize the Akaike Information Criterion
739 (AIC). We retrained our model weekly, using the entire history of positivity and epidemiolog-
740 ical data to date. We utilize an ex-post forecasting approach where we first project the next
741 week’s values of positivity by applying the ARIMA model to tweet positivity. The ARIMA
742 model is of a similar form to Eq. 5.3, except that positivity is the outcome value and the $\beta_1 \bar{P}_t$
743 term is excluded. Following this we used the ARIMA model to forecast cases and hospitaliza-
744 tions considering the ARIMA linearized relationship between the history of epidemiological
745 factors and tweet positivity and the projected values of positivity. Equivalently, without
746 altering the ARIMA structural form in Eq. 5.3, we predicted new hospitalization considering
747 different predictands, i.e. tweet volume, volume and positivity, or hospitalization only to
748 select the optimal model with the highest prediction accuracy.

749 **5.4.2 Geostatistical forecasting**

750 We predicted the spatial spread of healthcare pressure with geostatistical kriging consider-
 751 ing the inferred linear relationship between positivity and cumulative hospitalization at the
 752 city scale. This relationship is linked to the β_1 exponent in the ARIMA model of Eq. 5.3
 753 and is updated every week. A similar modeling was performed in the past by Berke (2004).
 754 Geostatistical kriging was performed using the `automap` package (Hiemstra et al., 2008).
 755 We restricted data to the most recent two weeks of tweets and cumulative hospitalization
 756 to ensure that there was enough geo-spatial tweet data salient to predict the last observed
 757 hospitalization. This was also supported by the limited “memory” of positivity for hospi-
 758 talization, reflected by low values of the ARIMA parameters p and d . As with the double
 759 step prediction of ARIMA, first we extrapolate positivity over the whole geographical do-
 760 main and after we perform a second geokriging to predict new hospitalization based on the
 761 positivity-hospitalization relationship. Given the limited volume of geo-located tweets, we
 762 used ordinary geo-statistical kriging because average is likely constant (Liang et al., 2018)
 763 (as in our case) to interpolate positivity using the semi-variogram:

$$\gamma_P(\delta) = \frac{1}{2N(\delta)} \left\{ \sum_{i=1}^{N(\delta)} [P_{i+\delta} - P_i]^2 \right\} \quad (5.4)$$

764

$$\hat{P}_j = \sum_{i=1}^M \lambda_i(P_j) \cdot P_i \quad (5.5)$$

765 where $\lambda_i(P_j)$ is a kriging weighting factor for the know value of the variable P at a sampled
 766 location i and $j \neq i$. A function is a semivariogram only if it is a conditionally negative
 767 definite function, i.e. for all weights $\lambda_1, \dots, \lambda_M$ subject to $\sum_{i=1}^M \lambda_i(P_j) = 0$ and locations
 768 i, \dots, M it holds: $\sum_{i,j=1}^M \lambda_i \gamma_P(i, j) \lambda_j$. This establishes the connection between predictions of
 769 Eq. 5.5. and semivariogram of Eq. 5.4. The experimental semi-variogram of the data at the
 770 observation location is fitted against a theoretical semi-variogram model of $\hat{\gamma}_P(\delta_P)$; the latter
 771 is an exponential, Gaussian or spherical semivariogram. One is thus making a distinction
 772 between the experimental variogram that is a visualization of the observed possible spatio-
 773 temporal correlation and the variogram model that is further used to define the weights of
 774 the kriging function on which predictions are based. M is the number of (10,000) randomly
 775 generated points which are interpolated using the kriging weighting factor $\lambda_i(P_j)$ determined
 776 by the semivariogram.

777 Next, we applied universal geostatistical kriging (Falah et al., 2017) to interpolate the

778 expected hospitalization \hat{H} over space considering the forecast based on the relationship
779 between twitter positivity and the state-level cumulative hospitalization. Universal kriging
780 is used because it assumes that the average is not constant as it is in our case. This is done
781 by using the following analytics:

$$\hat{\gamma}_H(\delta) = \frac{1}{2N(\delta)} \sum_{i=1}^{N(\delta)} [(\hat{H}_{i+\delta} - m) - (\hat{H}_i - m)]^2 \quad (5.6)$$

782

$$\hat{H}_j = m + \sum_{i=1}^M \lambda_i(H_j) \cdot (\hat{H}_i - m) \quad (5.7)$$

783 where $\hat{\gamma}_H(\delta)$ is the predicted semivariogram of expected positivity based on $m(\hat{P}) =$
784 $\sum_{l=0}^L \alpha_l f_l(\hat{P})$ that is a slow and continuous trend function (Kambhammettu et al., 2011)
785 capturing the linear relationship between hospitalization and tweet positivity among points
786 l ; these points may be different from the whole set of points M over which interpolation is
787 performed. Finally, to determine the healthcare pressure H_P at each point i we used

$$H_{P_i} = \begin{cases} \hat{H}_i - \langle \hat{H}_T \rangle = \hat{H}_i - \frac{\sum_{i=1}^M \hat{H}_i}{M} & \text{if } > 0 \\ 0 & \text{otherwise} \end{cases} \quad (5.8)$$

788 where $\langle \hat{H}_T \rangle$ is the expected average of hospitalization over the selected geographical do-
789 main, and M is the number of interpolated points. We applied the same model to spatially
790 explicit hospital bed occupancy in order to compare interpolations of hospitalization based
791 on state and hospital level data.

792

793 5.5 Predictability Indicators

794 Weekly indices are introduced to monitor the evolution of the pandemic, the short- and
795 long-term predictability of Twitter positivity and the departure between forecasts and ob-
796 servations. The *Risk Index* is set to measure the rate of change in epidemiological values,
797 yet in formulating indication of epidemic trends. The *Gap Index* is introduced as the differ-
798 ence between forecast predictions and observations normalized to previous observations. The
799 *Correlation Index* is calculated by estimating the Pearson correlation coefficient to quantify
800 the short-term forecast ability of positivity for epidemiological variables (new hospitaliza-
801 tions and new cases) via geokriging over space and via ARIMA over time. The first ARIMA

802 component and geokriging factors are linear functions of the linearized relationship between
803 positivity and epidemiological variables (Eqs. 5.3 and 5.7). To quantify the long-term pre-
804 dictability of highly diverging events, transfer entropy is introduced as the *Predictability Index*
805 that informs about the probabilistic predictability of positivity for epidemiological patterns
806 in terms of probability distribution functions rather than time point values. All indices are
807 analytically defined as:

$$R(Y_t) = (y_t - y_{t-1})/y_{t-1} = \Delta Y(\delta t)/100 \quad (5.9)$$

$$G(Y_t) = \hat{y}(t) - y(t)/y(t) = \Delta \hat{Y}_t/100 \quad (5.10)$$

$$\text{corr}(P, Y) = \frac{\sum_{t=1}^L (p_t - \bar{P})(y_t - \bar{Y})}{\sqrt{\sum_{t=1}^L (p_t - \bar{P})^2 \sum_{t=1}^L (y_t - \bar{Y})^2}} \quad (5.11)$$

$$TE_{P \rightarrow Y} = \sum p(Y_t, Y_{t-1}, P_{t-1}) \cdot \log \left(\frac{p(Y_t|Y_{t-1}, P_{t-1})}{p(Y_t|Y_{t-1})} \right) \quad (5.12)$$

808 where $Y = I$ or ΔH is indicating time series of cases or hospitalization, respectively,
809 and y indicates time point values. $\bar{P} = \frac{1}{L} \sum_{t=1}^L p_t$ and $\bar{Y} = \frac{1}{L} \sum_{t=1}^L y_t$. L is the length of
810 time-series of P and Y .

811 The Value of Misinformation (*VoMi*) was defined as the difference of gap indices as:

$$VoMi(t) = G(Y_t)_S - G(Y_t)_M \quad (5.13)$$

812 where S and M stand for the systemic Twitter information and classified misinformation
813 set in predicting Y as cases or hospitalization. *VoMi* provides users with a measure of how
814 misinformation impact forecasts of epidemiological variables with respect to the systemic
815 tweet information considering both model and data uncertainty contained in the gap index.

816 Increasing values of *VoMi* (independently of the sign) indicate that the misinformation
817 tweet subset has increasing importance in forecasting versus the full tweet set. On average,
818 if *VoMi* is positive, misinformation does contribute non-negligibly to overpredict epidemio-
819 logical trends, whereas if it is negative it impacts positively and substantially the forecasts
820 proportionally to the magnitude of the misinformation gap $G(Y_t)_M$. This is evaluated for
821 the same model structure and epidemiological data uncertainty of the full tweet information.
822 It should be noted that both gap indices $G(Y_t)_S$ and $G(Y_t)_M$ can be negative and $M \subseteq S$,
823 yet the relative (non-linear) balance between full information and misinformation (positivity)

824 predictability contribute to determining VoMi.

825 In a decision analytical sense VoMi is defined as the amount of resources a decision
826 maker would be willing to pay for extra information that increase forecast accuracy be-
827 fore an event occurs. The optimal information set \mathbf{I}_{opt} is defined as the one whose gap is
828 minimized (assuming that data are perfect “error-free” information to match) and equal to
829 $G(\mathbf{I}_{opt}) = G(\mathbf{I}_{sub}) - VoMi(\mathbf{I}_{opt}, \mathbf{I}_{sub})$ where $VoMi = MI(P, H)$ that is the mutual informa-
830 tion $MI(P, Y) = \sum_p \sum_y p(p, y) \log \frac{p(p, y)}{p(p)p(y)}$ between positivity and cases or hospitalization.
831 Mutual Information in an information-theoretic variable measuring the amount of information
832 shared between two variables that is on average inversely proportional to the predictability
833 indicator in Eq. 5.12 (i.e. the uncertainty reduction between variables).

834 5.6 Tweet Spread

835 For each week, we calculated and displayed the average daily tweet and retweet volume for all
836 tweets and the misinformation related tweets. Time series of tweet and retweet volumes, as
837 well as their corresponding average positivity, are displayed by InTo, which serve as indicators
838 of spreading potential of COVID-19 related messages within and beyond the geographical
839 domain considered. Additionally, the Twitter user of the most popular tweet in a week is
840 shown when hovering over a point on the Tweet spread plot.

841 5.7 Dashboard Architecture

842 The InTo dashboard utilizes a client-server architecture designed and implemented using the
843 `shiny` package (Chang et al., 2020) in R (R Core Team, 2020) that provides a convenient
844 wrapper for interactive HTML widgets. This is similar to GLEaMviz architecture (Van den
845 Broeck et al., 2011). The client component only allows users to visualize the results of InTo
846 but many outputs, for example predictability indicators, are downloadable by users. All
847 computations on the server are conducted in R using the established workflow (see Fig. 1).

848 InTo online

849 InTo online dashboards and data are at:

850 https://nexuslab.shinyapps.io/InTo_Delhi/ for the city of New Delhi

851 https://nexuslab.shinyapps.io/InTo_Mumbai/ for the city of Mumbai

852 https://nexuslab.shinyapps.io/InTo_Jakarta/ for the city of Jakarta

853 https://nexuslab.shinyapps.io/InTo_Bangkok/ for the city of Bangkok

854

855 Into online manual, workflow, data sources and codes is at:

856 <https://rpubs.com/elroyg1/Into-walkthrough>

857

858 Into main code is at:

859 <https://github.com/elroyg1/InTo>

860

861 **Data Ethical Approval**

862 Twitter data are collected by leveraging Twitter’s free streaming API. A Twitter developer
863 account was obtained as well as the necessary authentication tokens. The data set is avail-
864 able in compliance with the Twitter’s Terms and Conditions ([https://developer.twitter.](https://developer.twitter.com/en/developer-terms/agreement-and-policy)
865 [com/en/developer-terms/agreement-and-policy](https://developer.twitter.com/en/developer-terms/agreement-and-policy)), under which we are unable to publicly
866 release the text of the collected tweets. Twitter developer account was obtained on May
867 7, 2020. We are, therefore able to release Tweet IDs, which are unique identifiers tied to
868 specific tweets. The Tweet IDs can be used by researchers to query Twitter’s API and obtain
869 the complete tweet object, including tweet content (text, URLs, hashtags, etc) and authors’
870 metadata. Our collection relies upon publicly available data (both epidemiological and Twit-
871 ter data) and is hence registered as IRB (institutional review board) exempt by Hokkaido
872 University.

873 **Author Contribution**

874 E.G. performed all calculations and data mining, developed the dashboard, and contributed
875 to the writing.

876 J.L. supported the data mining and performed predictability index calculations.

877 M.C. conceptualized, analytically formalized, designed and guided the dashboard creation,
878 and wrote the manuscript.

879

880 **Acknowledgements**

881 All authors acknowledge the collaboration and support from SEARO/WHO (project num-
882 ber 2020/1015441-0). Victor del Rio-Vilas at WHO/SEARO is greatly acknowledged. E.G.
883 acknowledges the Ministry of Education, Culture, Sports, Science and Technology (MEXT)
884 for this PhD fellowship. M.C. acknowledges the funding from the FY2020 SOUSEI Support
885 Program and Award for Young Researchers (awarded by the Executive Office for Research
886 Strategy to the Top 20% scientists in terms of productivity and citations at Hokkaido Uni-
887 versity) and the GI-CoRE GSB Station at Hokkaido University, Sapporo, Japan.

888 References

- 889 Susel Góngora Alonso, Isabel de la Torre Díez, and Begoña García Zapirain. Predictive, per-
890 sonalized, preventive and participatory (4p) medicine applied to telemedicine and ehealth
891 in the literature. Journal of medical systems, 43(5):140, 2019.
- 892 Joana M Barros, Jim Duggan, and Dietrich Rebholz-Schuhmann. The application of internet-
893 based sources for public health surveillance (infoveillance): systematic review. Journal of
894 Medical Internet Research, 22(3):e13680, 2020.
- 895 Olaf Berke. Exploratory disease mapping: kriging the spatial risk function from regional
896 count data. International Journal of Health Geographics, 3(1):18, 2004.
- 897 Nicola Luigi Bragazzi. Infodemiology and infoveillance of multiple sclerosis in italy. Multiple
898 sclerosis international, 2013, 2013.
- 899 Winston Chang, Joe Cheng, JJ Allaire, Yihui Xie, and Jonathan McPherson. shiny: Web
900 Application Framework for R, 2020. URL <https://CRAN.R-project.org/package=shiny>.
901 R package version 1.4.0.2.
- 902 Peter Sheridan Dodds, Kameron Decker Harris, Isabel M Kloumann, Catherine A Bliss, and
903 Christopher M Danforth. Temporal patterns of happiness and information in a global
904 social network: Hedonometrics and twitter. PloS one, 6(12):e26752, 2011.
- 905 Maeve Duggan and Joanna Brenner. The demographics of social media users, 2012, vol-
906 ume 14. Pew Research Center’s Internet & American Life Project Washington, DC, 2013.
- 907 Johannes C Eichstaedt, Hansen Andrew Schwartz, Margaret L Kern, Gregory Park, Darwin R
908 Labarthe, Raina M Merchant, Sneha Jha, Megha Agrawal, Lukasz A Dziurzynski, Maarten
909 Sap, et al. Psychological language on twitter predicts county-level heart disease mortality.
910 Psychological science, 26(2):159–169, 2015.
- 911 Gunther Eysenbach. Infodemiology and infoveillance: framework for an emerging set of public
912 health informatics methods to analyze search, communication and publication behavior on
913 the internet. Journal of medical Internet research, 11(1):e11, 2009.
- 914 Annisa Nur Falah, Betty Subartini, and Budi Nurani Ruchjana. Application of universal
915 kriging for prediction pollutant using gstat r. In IOP Conf. Series: Journal of Physics:
916 Conf. Series, volume 893, pages 1–7, 2017.
- 917 Riccardo Gallotti, Francesco Valle, Nicola Castaldo, Pierluigi Sacco, and Manlio
918 De Domenico. Assessing the risks of” infodemics” in response to covid-19 epidemics. arXiv
919 preprint arXiv:2004.03997, 2020.

920 Jeremy Ginsberg, Matthew H Mohebbi, Rajan S Patel, Lynnette Brammer, Mark S Smolin-
921 ski, and Larry Brilliant. Detecting influenza epidemics using search engine query data.
922 Nature, 457(7232):1012–1014, 2009.

923 Pari Delir Haghighi, Yong-Bin Kang, Rachele Buchbinder, Frada Burstein, and Samuel Whit-
924 tle. Investigating subjective experience and the influence of weather among individuals with
925 fibromyalgia: a content analysis of twitter. JMIR public health and surveillance, 3(1):e4,
926 2017.

927 P.H. Hiemstra, E.J. Pebesma, C.J.W. Twenh”ofel, and G.B.M. Heuvelink. Real-
928 time automatic interpolation of ambient gamma dose rates from the dutch ra-
929 dioactivity monitoring network. Computers & Geosciences, 2008. DOI:
930 <http://dx.doi.org/10.1016/j.cageo.2008.10.011>.

931 Md Saiful Islam, Tonmoy Sarkar, Sazzad Hossain Khan, Abu-Hena Mostofa Kamal, Sarkar
932 Mohammad Murshid Hasan, Alamgir Kabir, Dalia Yeasmin, Mohammad Ariful Islam,
933 Kamal Ibne Amin Chowdhury, Kazi Selim Anwar, Abrar Ahmad Chughtai, and Holly
934 Seale. Covid-19?related infodemic and its impact on public health: A global social media
935 analysis. The American Society of Tropical Medicine and Hygiene, 2020.

936 Shan Jiang and Christo Wilson. Linguistic signals under misinformation and fact-
937 checking: Evidence from user comments on social media. Proceedings of the ACM on
938 Human-Computer Interaction, 2(CSCW):1–23, 2018.

939 BVNP Kambhammettu, Praveena Allena, and James P King. Application and evaluation of
940 universal kriging for optimal contouring of groundwater levels. Journal of Earth System
941 Science, 120(3):413, 2011.

942 Michael W. Kearney. rtweet: Collecting and analyzing twitter data. Journal of Open Source
943 Software, 4(42):1829, 2019. doi: 10.21105/joss.01829. URL [https://joss.theoj.org/](https://joss.theoj.org/papers/10.21105/joss.01829)
944 [papers/10.21105/joss.01829](https://joss.theoj.org/papers/10.21105/joss.01829). R package version 0.7.0.

945 Devakumar kp. covid-19-india-data, 2020. URL [https://github.com/imdevskp/](https://github.com/imdevskp/covid-19-india-data)
946 [covid-19-india-data](https://github.com/imdevskp/covid-19-india-data).

947 J Li and M Convertino. Taming network inference: Optimal information flow model. PNAS,
948 2020. in review.

949 Quanzhi Li, Qiong Zhang, Luo Si, and Yingchi Liu. Rumor detection on social media:
950 Datasets, methods and opportunities. arXiv preprint arXiv:1911.07199, 2019.

951 Ching-Ping Liang, Jui-Sheng Chen, Yi-Chi Chien, and Ching-Fang Chen. Spatial analysis of
952 the risk to human health from exposure to arsenic contaminated groundwater: A kriging
953 approach. Science of The Total Environment, 627:1048–1057, 2018.

954 Yang Liu, Brenda O Hoppe, and Matteo Convertino. Threshold evaluation of emergency risk
955 communication for health risks related to hazardous ambient temperature. Risk analysis,
956 38(10):2208–2221, 2018.

957 Savi Maharaj and Adam Kleczkowski. Controlling epidemic spread by social distancing: Do
958 it well or not at all. BMC Public Health, 12(1):679, 2012a.

959 Savi Maharaj and Adam Kleczkowski. Controlling epidemic spread by social distancing: Do
960 it well or not at all. BMC Public Health, 12(1):679, 2012b.

961 Craig J McGowan, Matthew Biggerstaff, Michael Johansson, Karyn M Apfeldorf, Michal
962 Ben-Nun, Logan Brooks, Matteo Convertino, Madhav Erraguntla, David C Farrow, John
963 Freeze, et al. Collaborative efforts to forecast seasonal influenza in the united states,
964 2015–2016. Scientific reports, 9(1):1–13, 2019.

965 Jonathan Mellon and Christopher Prosser. Twitter and facebook are not representative of
966 the general population: Political attitudes and demographics of british social media users.
967 Research & Politics, 4(3):2053168017720008, 2017.

968 Saif Mohammad and Peter Turney. Emotions evoked by common words and phrases: Using
969 mechanical turk to create an emotion lexicon. In Proceedings of the NAACL HLT 2010
970 workshop on computational approaches to analysis and generation of emotion in text, pages
971 26–34, 2010.

972 Danielle Mowery, Hilary Smith, Tyler Cheney, Greg Stoddard, Glen Coppersmith, Craig
973 Bryan, and Mike Conway. Understanding depressive symptoms and psychosocial stressors
974 on twitter: a corpus-based study. Journal of medical Internet research, 19(2):e48, 2017.

975 Mitchell O’Hara-Wild, Rob Hyndman, and Earo Wang. fable: Forecasting Models for Tidy
976 Time Series, 2020. URL <https://CRAN.R-project.org/package=fable>. R package ver-
977 sion 0.2.1.

978 A Ross Otto and Johannes C Eichstaedt. Real-world unexpected outcomes predict city-level
979 mood states and risk-taking behavior. PloS one, 13(11):e0206923, 2018.

980 Michael J Paul, Mark Dredze, and David Broniatowski. Twitter improves influenza forecast-
981 ing. PLoS currents, 6, 2014.

982 R Core Team. R: A Language and Environment for Statistical Computing. R Foundation
983 for Statistical Computing, Vienna, Austria, 2020. URL <https://www.R-project.org/>.

984 M Radin and S Sciascia. Infodemiology of systemic lupus erythematosus using google trends.
985 Lupus, 26(8):886–889, 2017.

986 Sudha Ram, Wenli Zhang, Max Williams, and Yolande Pengetnze. Predicting asthma-
987 related emergency department visits using big data. IEEE journal of biomedical and health
988 informatics, 19(4):1216–1223, 2015.

989 Tyler W. Rinker. qdap: Quantitative Discourse Analysis Package. Buffalo, New York, 2020.
990 URL <http://github.com/trinker/qdap>. 2.3.6.

991 Marco Rocchetti, Gustavo Marfia, Paola Salomoni, Catia Prandi, Rocco Maurizio Zagari,
992 Faustine Linda Gningaye Kengni, Franco Bazzoli, and Marco Montagnani. Attitudes of
993 crohn?s disease patients: Infodemiology case study and sentiment analysis of facebook and
994 twitter posts. JMIR public health and surveillance, 3(3):e51, 2017.

995 Shouq A Sadah, Moloud Shahbazi, Matthew T Wiley, and Vagelis Hristidis. A study of the
996 demographics of web-based health-related social media users. Journal of medical Internet
997 research, 17(8):e194, 2015.

998 Takeshi Sakaki, Makoto Okazaki, and Yutaka Matsuo. Earthquake shakes twitter users: real-
999 time event detection by social sensors. In Proceedings of the 19th international conference
1000 on World wide web, pages 851–860, 2010.

1001 Mauricio Santillana, André T Nguyen, Mark Dredze, Michael J Paul, Elaine O Nsoesie,
1002 and John S Brownstein. Combining search, social media, and traditional data sources to
1003 improve influenza surveillance. PLoS Comput Biol, 11(10), 2015.

1004 Juan Carlos Medina Serrano, Orestis Papakyriakopoulos, and Simon Hegelich. Nlp-based
1005 feature extraction for the detection of covid-19 misinformation videos on youtube, 2020.

1006 Julia Silge and David Robinson. tidytext: Text mining and analysis using tidy data principles
1007 in r. JOSS, 1(3), 2016. doi: 10.21105/joss.00037. URL [http://dx.doi.org/10.21105/](http://dx.doi.org/10.21105/joss.00037)
1008 [joss.00037](http://dx.doi.org/10.21105/joss.00037).

1009 Laura Silver, Christine Huang, and Kyle Taylor. In emerging economies smart phone and
1010 social media users have broader social networks. Pew Research Center, 2019.

1011 Linda Thunström, Stephen C Newbold, David Finnoff, Madison Ashworth, and Jason F
1012 Shogren. The benefits and costs of using social distancing to flatten the curve for covid-19.
1013 Journal of Benefit-Cost Analysis, pages 1–27, 2020.

- 1014 Carolina Oi Lam Ung. Community pharmacist in public health emergencies: quick to ac-
1015 tion against the coronavirus 2019-ncov outbreak. Research in Social and Administrative
1016 Pharmacy, 2020.
- 1017 Wouter Van den Broeck, Corrado Gioannini, Bruno Gonçalves, Marco Quaggiotto, Vittoria
1018 Colizza, and Alessandro Vespignani. The gleamviz computational tool, a publicly avail-
1019 able software to explore realistic epidemic spreading scenarios at the global scale. BMC
1020 infectious diseases, 11(1):1–14, 2011.
- 1021 Aditya Vashistha, Edward Cutrell, Nicola Dell, and Richard Anderson. Social media plat-
1022 forms for low-income blind people in india. In Proceedings of the 17th International ACM
1023 SIGACCESS Conference on Computers & Accessibility, pages 259–272, 2015.
- 1024 Victor Del Rio Vilas, M Kocaman, Howard Burkom, Richard Hopkins, John Berezowski, Ian
1025 Painter, Julia Gunn, G Montibeller, M Convertino, LC Streichert, et al. A value-driven
1026 framework for the evaluation of biosurveillance systems. Online Journal of Public Health
1027 Informatics, 9(1), 2017.
- 1028 WHO et al. 2019 novel coronavirus (2019-ncov): strategic preparedness and response plan,
1029 2020.
- 1030 Max L Wilson, Susan Ali, and Michel F Valstar. Finding information about mental health in
1031 microblogging platforms: a case study of depression. In Proceedings of the 5th Information
1032 Interaction in Context Symposium, pages 8–17, 2014a.
- 1033 Max L. Wilson, Susan Ali, and Michel F. Valstar. Finding information about mental health in
1034 microblogging platforms: A case study of depression. In Proceedings of the 5th Information
1035 Interaction in Context Symposium, IiX '14, page 8?17, New York, NY, USA, 2014b. As-
1036 sociation for Computing Machinery. ISBN 9781450329767. doi: 10.1145/2637002.2637006.
1037 URL <https://doi.org/10.1145/2637002.2637006>.

1038 **Table Captions**

1039 **Table 1. Average Socio-epidemiological Values for New Delhi.** Average weekly val-
1040 ues for hospitalization H , cases I , tweet volume, retweet and positivity (V , R , and P), as well
1041 as Pearson correlation between positivity and hospitalization. Average $VoMi$ also provided.
1042 The Pearson correlation is proportional to the first regression coefficient of the ARIMA fore-
1043 casting model and the geokriging factor of hospitalization predictions. The higher $\text{corr}(P, H)$
1044 the higher the potential risk aversion for the city (areas and time periods) considered. It is
1045 empirically observed that the higher the risk aversion the lower the social (Twitter) genera-
1046 tion of information and the healthcare pressure defined by combined case and hospitalization
1047 magnitude. $VoMi$ is expected to be higher for less risk-averting city areas (and time periods)
1048 with higher incidence (thus misinformation is more predictive of cases and hospitalization)
1049 and these areas/time periods should appear more local in terms of circulating information.

1050

1051 **Figure Captions**

1052 **Figure 1. Conceptual and Computational Workflow of InTo.** The process begins
1053 with downloading both social media content and epidemiological data. Social media data is
1054 then disaggregated into content related to healthcare and misinformation, with the aggregated
1055 content retained for analysis as well. As for epidemiological data, the dashboard makes
1056 use of hospitalization and cases data for the disease considered. The next process is the
1057 extraction of features from social media content: for each subset, bi-grams, count informa-
1058 tion and sentiments are quantified. Metrics quantifying the relationships between sentiment
1059 and epidemiological data are then calculated. Once the linear regression coefficients are esti-
1060 mated, these are used to forecast the spatial and temporal variation of healthcare pressure,
1061 which is then visualized for users on the dashboard. To illustrate the process and output of
1062 InTo we examine the case of New Delhi, India.

1063

1064 **Figure 2. Dashboard Tab 1: Healthcare Pressure Spatial Predictions.** Users
1065 are presented with a heatmap, time series of tweet positivity, cases, new hospitalizations
1066 and cumulative hospitalizations. In addition, two text outputs inform the user about the
1067 predicted hospitalization and cases for the selected city and the difference between the cur-
1068 rent predicted values and the values predicted for last week. The heatmap visualizes the
1069 results of geokriging the spatial interpolation of hospitalization as a function of tweet posi-
1070 tivity. Hotter areas are where patients potentially in need of hospitalization are concentrated.

1071

1072 **Figure 3. Spatial Forecasts.** Gradients of Healthcare Pressure, that is $HP_i =$
1073 $\hat{H}_{T_i} - H_T$, reflect potential movement of people in need of hospitalization (hospitalization
1074 fluxes). The sum of HP_i from geokriging over space is theoretically equal to the predicted
1075 cumulative hospitalization over time ($H_T = \sum_t \Delta H(t)$) as a function of the new hospitaliza-
1076 tion (that are temporal hospitalization fluxes or healthcare pressure over time). An Effective
1077 Healthcare Pressure can be calculated as difference between normalized HP_i and healthcare
1078 capacity (HC_I) as a function of area healthcare infrastructure resources (e.g. beds, ICUs,
1079 ventilators). Uncertainty in forecasts can also consider spatially explicit testing rate and
1080 surveillance capacity. In analogy to weather forecasts, gradient of pressure over space are the
1081 byproduct of gradient of pressure over time modulated by underlying environmental condi-
1082 tions.

1083

1084 **Figure 4. Dashboard Tab 2: Emotions, Top Bigrams and Tweets for Pre-**
1085 **dictive Information, Misinformation and Healthcare.** In the Emotions and Misinfor-
1086 mation section, users are shown two time series of emotional affect, a table of tweet texts
1087 with their retweet counts and positivity, and a visualization of the top bigrams for a selected
1088 week. The time series on the left presents the absolute volume of emotional affects while the
1089 time series on the visualizes the proportional volume of each category. Users are given the
1090 opportunity to visualize the output for all tweets, or the subset of misinforming or healthcare
1091 tweets. They are also given the opportunity to select and send any tweet from the table to the
1092 administrators for inclusion in the misinformation subset of tweets. The administrators can
1093 redo the analysis of the impact and value of misinformation considering the newly identified
1094 misinforming tweets.

1095

1096 **Figure 5. Dashboard Tab 3: Predictability Indicators.** The Predictability section
1097 displays time series of risk, gap, predictability, and correlation indices along with the value
1098 of misinformation. In the left plots, users are shown these indices when the positivity of all
1099 tweets are used to forecast cases and hospitalizations. Middle plots show these indices when
1100 the positivity of the subset of misinforming tweets are used to forecast cases and hospital-
1101 izations. The right plots show times series of the value of misinformation (VoMi). For all
1102 plots, the x axis represents the time in weeks, while the y axis represents the value of the
1103 indicator as a percentage ratio. When users hover over a point, they are presented with the
1104 x-y coordinates.

1105

1106 **Figure 6. Dashboard Tab 3: Information Volume and Spreading Potential.**
1107 The Tweet Spread section visualizes the spreading potential considering all tweets and the
1108 spreading potential from the subset of misinforming tweets. The x axis represents time in
1109 weeks while the y axis indicates the tweet volume observed in that week. The dashed lines
1110 shows the tweet volume for all tweets in that category while the solid line indicates the volume
1111 for the most retweeted tweets. The size of each point represents the mean retweet volume for
1112 that week, while the color represents the positivity of the most retweeted tweet observed the
1113 selected week. By hovering over a point the most retweeted tweet for that week is presented
1114 on the right.

1115

1116 **Figure 7. Spatial Validation of Geokriging Predictions of Cumulative Hospi-**
1117 **talization.** Predicted and observed cumulative hospitalization (\hat{H}_T and H_T) are calculated

1118 as a function of spatially explicit positivity P_i and hospital reported hospitalization (plot A
1119 and C) via geokriging. Plot A shows the prediction offered by the dashboard where spatial
1120 healthcare pressure $HP_i = \hat{H}_{T_i} - H_T$ is determined as difference between local and total
1121 hospitalization at the city scale. Plot B and D report predictions of hospital location based
1122 on positivity and cumulative hospitalization based on reported bed occupancy only, respec-
1123 tively. The relationship on the top of each plot is reporting what is used in the geokriging
1124 calibration, while what is predicted is reported at the bottom. Squares indicate officially
1125 reported hospitals designated for COVID-19 patients, while blue points indicate geo-located
1126 Tweets. Predictions are for the period 21 July-11 August 2020.

1127

1128 **Figure 8. Hospitalization and Case Forecasting for Different Predictive Mod-**
1129 **els.** The results of ARIMA forecasts with different models in terms of predictors are shown
1130 for cases, cumulative and new hospitalization (top to bottom) for New Delhi. ACF is ARIMA
1131 based on epidemiological data only, while all other ARIMA models are based on positivity,
1132 Tweet volume, Tweet volume and positivity combined (red, blue, yellow, and green curves).
1133 Black dots are from observations at the city scale. All curves are at the daily resolution.

1134

City	\bar{H}_t	\bar{I}_t	\bar{V}_t	\bar{R}_t	\bar{P}_t	$\text{corr}(P, H)$	$VoMi$
New Delhi	100	1000	10,600	9	5.75	-0.5	0.00
Mumbai	500	1250	10,500	10	5.85	-0.1	0.10
Bangkok	1	4	1000	11	5.80	-2	-0.05
Jakarta	25	200	900	20	5.90	-1	-0.10

Table 1:

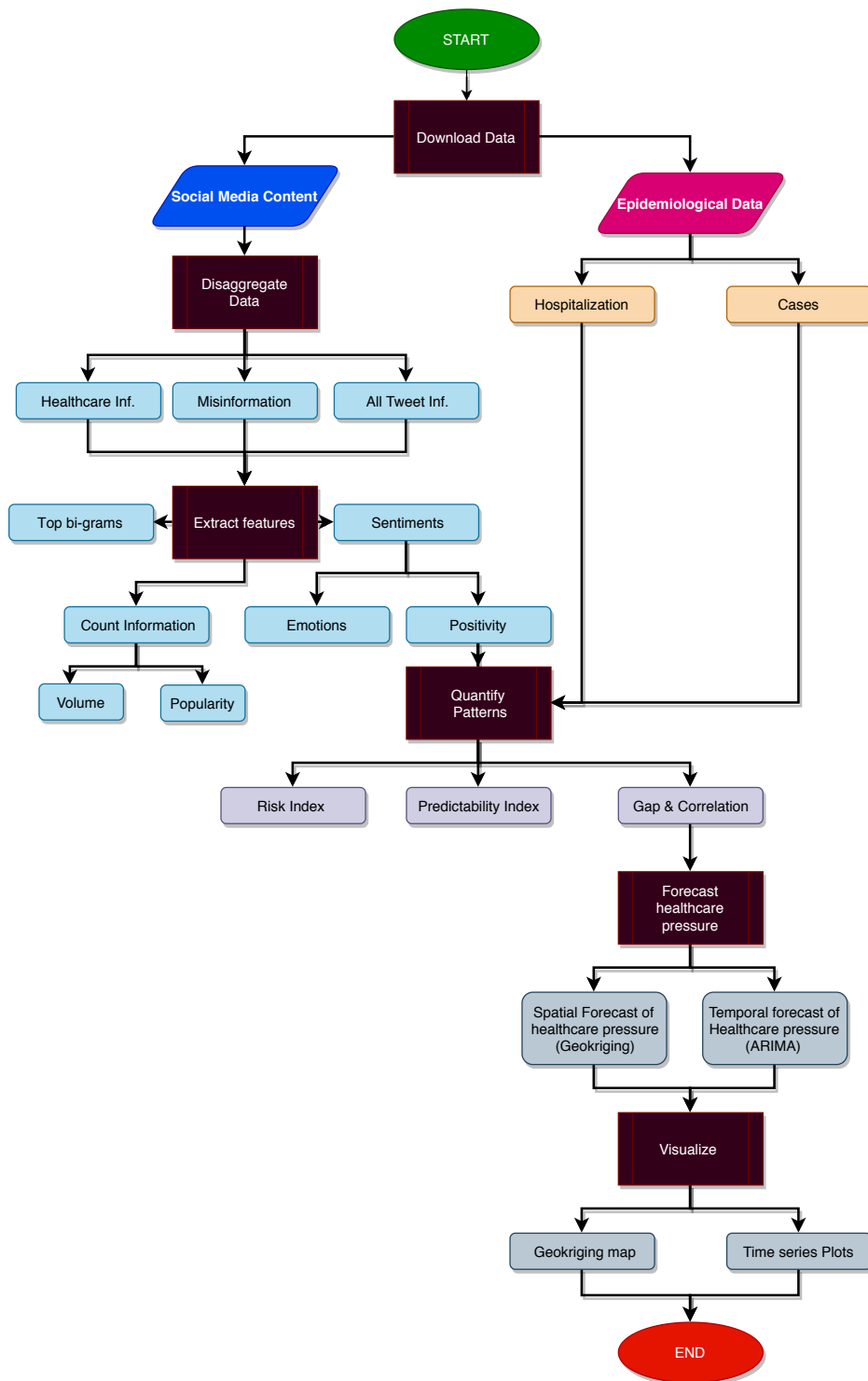


Figure 1:

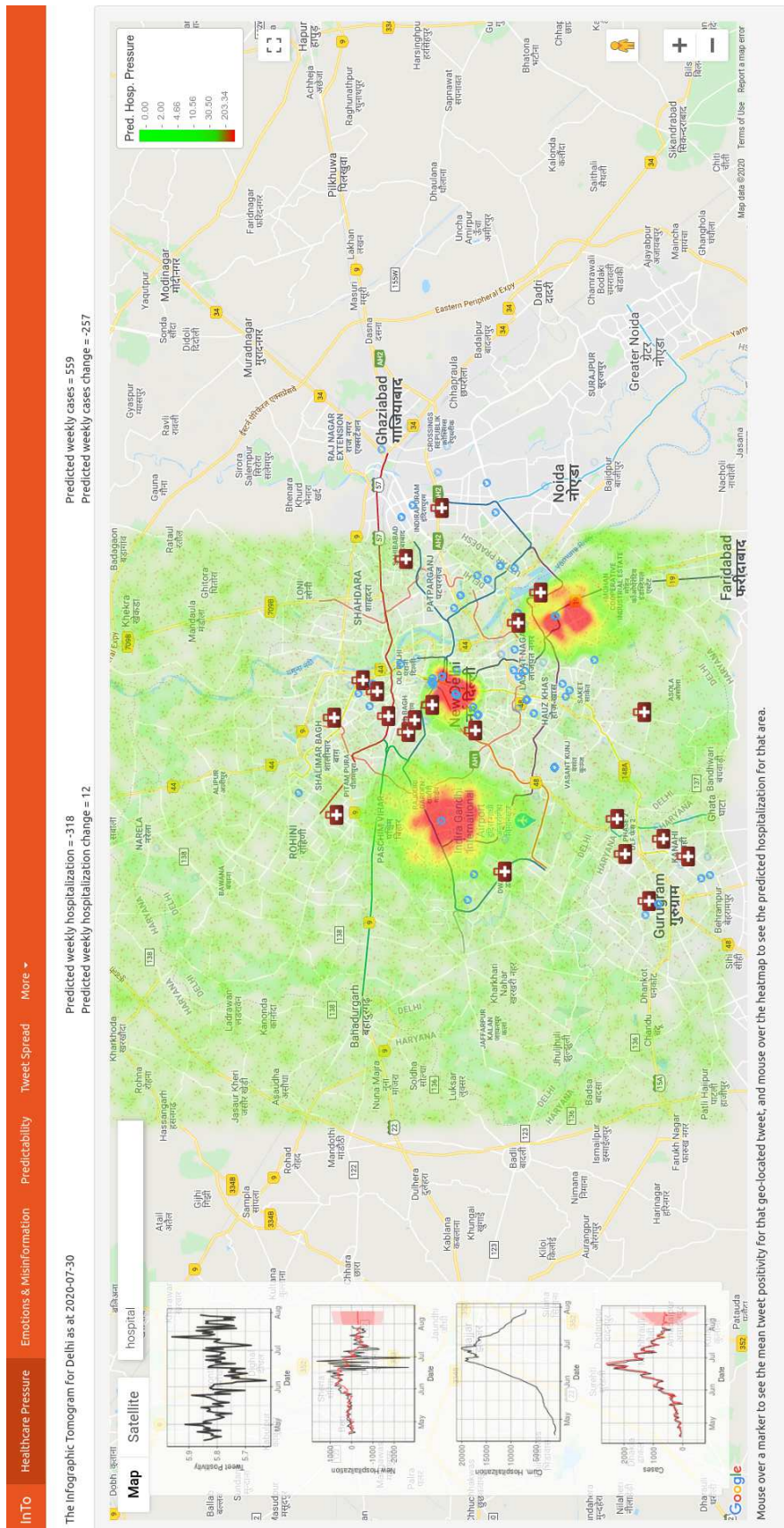


Figure 2:

The Infographic Tomogram for Delhi as at 2020-07-16

Predicted weekly hospitalization = -382
 Predicted weekly hospitalization change = 21

Predicted weekly cases = 1400
 Predicted weekly cases change = -143

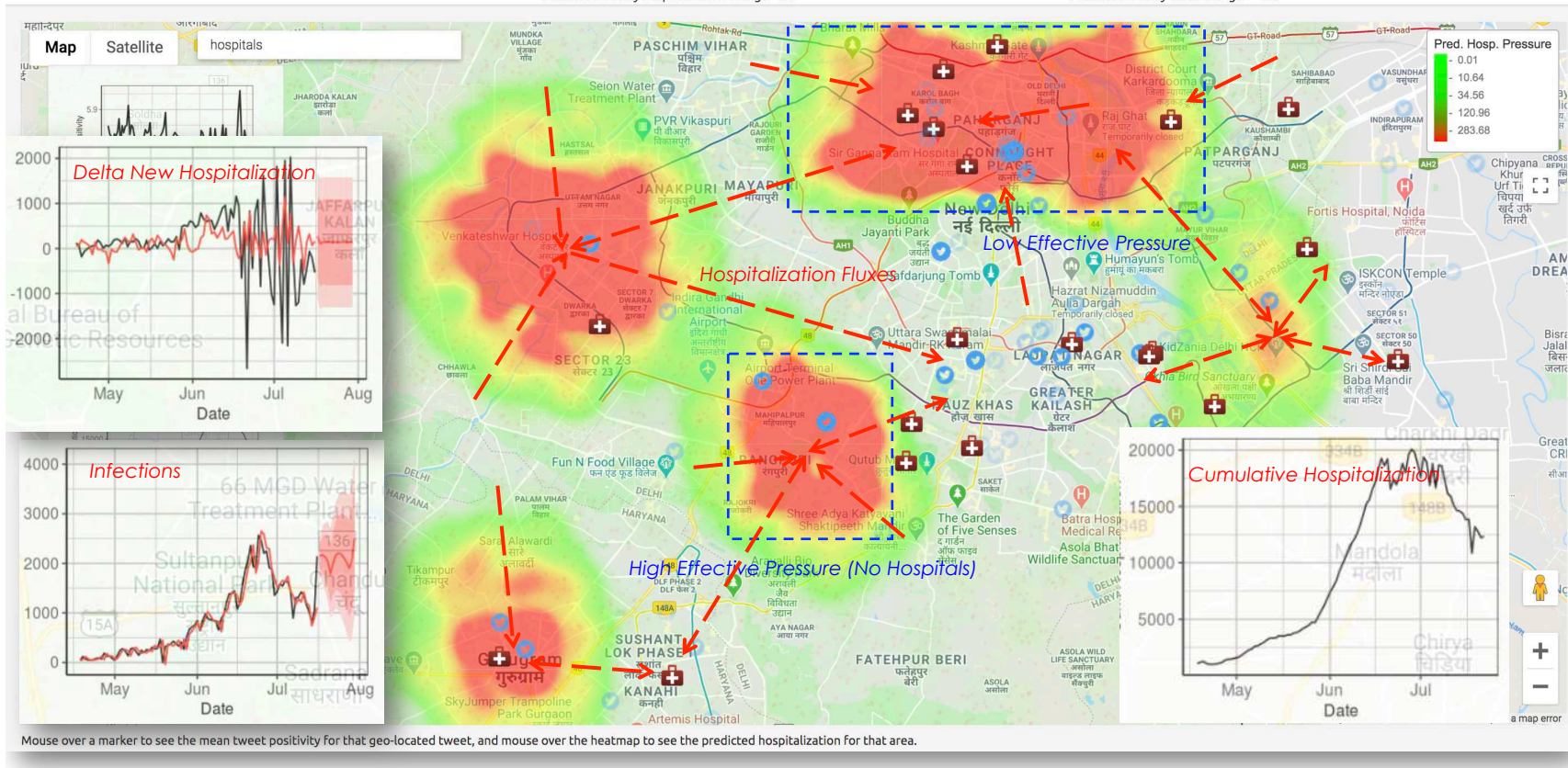


Figure 3:

Date	User	Tweet	Retweet Count	Positivity
2020-07-17	shashank_sjs	Shankacharya was detained on Dholew, that too on false charges. Then why is this unnecessary delay in arresting Bishop Franco Mulakkal in such a serious issue? https://t.co/9NvFbA2Bz8	231	3.34
2020-08-08	subindemis	Latest fake news from corporate media in Kerala: 1) 5 dams collapsed - Manorama. (Fact: shutters of 5 dams opened) 2) 4-year-old child in #Kozhikode flight has died - Manorama. (Fact: she is alive) 3) 40 ppl in flight have COVID-19 - Mathrubhumi. (Fact: 1 has COVID so far)	186	5.41
2020-08-08	subindemis	Latest fake news from corporate media in Kerala: 1) 5 dams collapsed - Manorama. (Fact: shutters of 5 dams opened) 2) 4-year-old child in #Kozhikode flight has died - Manorama. (Fact: she is alive) 3) 40 ppl in flight have COVID-19 - Mathrubhumi. (Fact: 1 has COVID so far)	186	5.41
2020-07-20	Opindia_com	Bengaluru police arrest one Sameer Ullah for triggering panic via fake video claiming to be from COVID hospital https://t.co/AspNkGuvz1	147	3.55
2020-07-21	kavita_krishnan	To the list of political prisoners who got Covid-19 while imprisoned on false charges in Maharashtra, add 50 more. Maharashtra is a life-threatening danger because the Modi regime is weaponising the pandemic to turn prisons into death camps for political undertrial prisoners. https://t.co/08UllBGFx	117	3.59
2020-07-21	CongressSevudal	In Karnataka, dead bodies were dumped in pits due to fear and misinformation about those who die of Covid-19. Congress MP From Bengaluru Rural Shri D K Suresh gave an elderly man who died of the virus a respectful final adieu to dispel such baseless fears. https://t.co/2Hsrjhe4d	97	3.2
2020-07-17	kavita_krishnan	The world needs to be awakened to the crime against humanity, where Covid-19 is being used by the Government of India to target false allegations under draconian laws, into veritable death sentences for political prisoners. @amrigholiver @mehdirhasan @hasanminhaj @AOC	93	4.06
2020-08-03	PTL_News	About 2,300 people who tested positive for COVID-19 in Lucknow gave false information pertaining to their names, mobile numbers and addresses: UP Health official	90	6.18
2020-08-03	PTL_News	About 2,300 people who tested positive for COVID-19 in Lucknow gave false information pertaining to their names, mobile numbers and addresses: UP Health official	90	6.18
2020-07-27	timesofindia	Out of job due to #COVID19 situation, Hyderabad techie starts selling vegetables; says she doesn't believe in 'false prestige' https://t.co/X6MYS2u1w6 https://t.co/ILWFOuJelb	80	4.98

Search:

Previous 1 2 3 4 5 ... 48 Next

Please select and send tweets with misinformation

Send

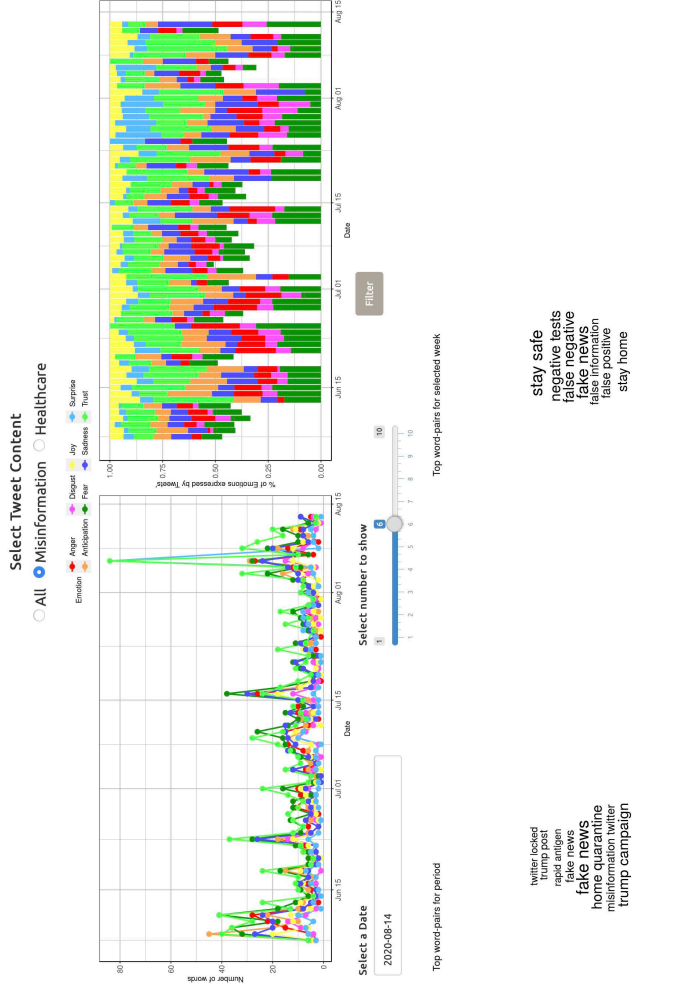


Figure 4:

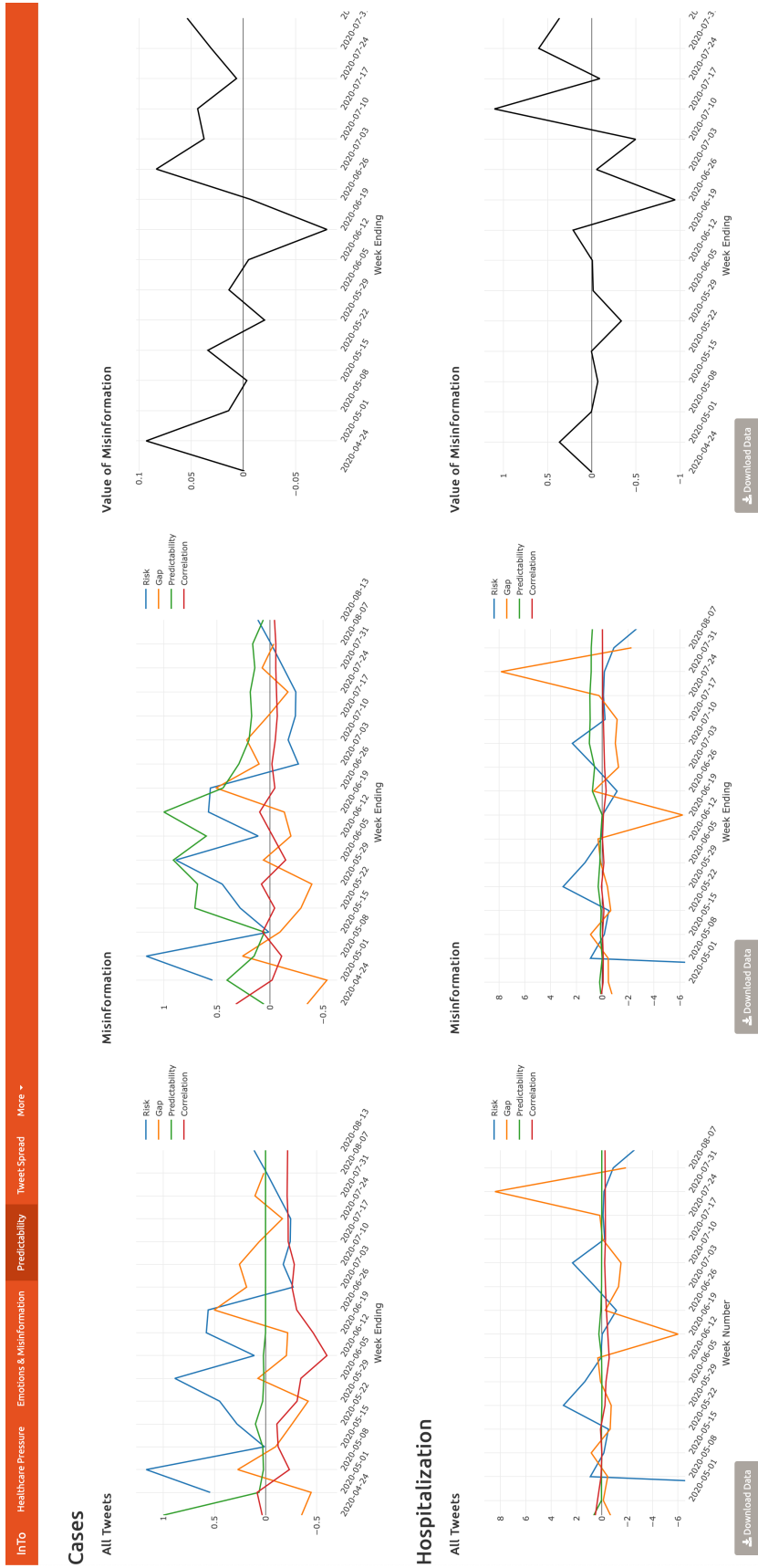
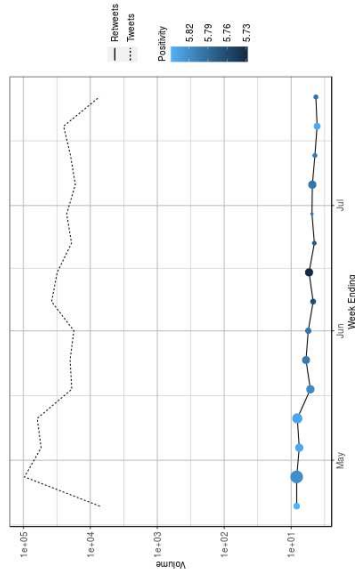


Figure 5:

All Tweets

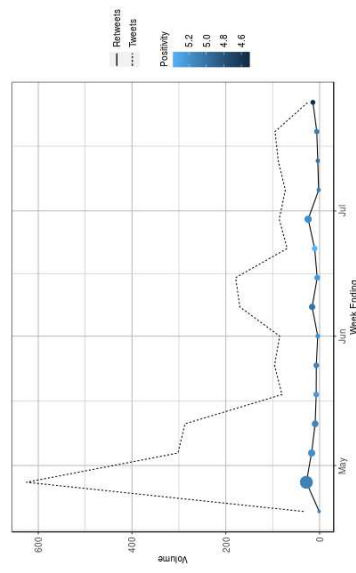


Most Popular Tweet

Delhi Govt requests #TablighiJamaat members who have recovered from #COVID to donate plasma for other patients. T.J members readily agree! They're literally giving their blood to cure others but no TV news channel will talk about this #Covid_19India #PlasmaTherapy #ramadankareem

Click a point on the chart to see the most popular tweet

Misinformation



Most Popular Tweet

Arbab Goswami has resigned from Editor's Guild, which has no credibility left, and its bias is not even subtle. Not even a word on #PaighatLynching by the Guild. They have been silent on fake news stories during COVID. Courage to speak truth is absent. #ArbabGoswami

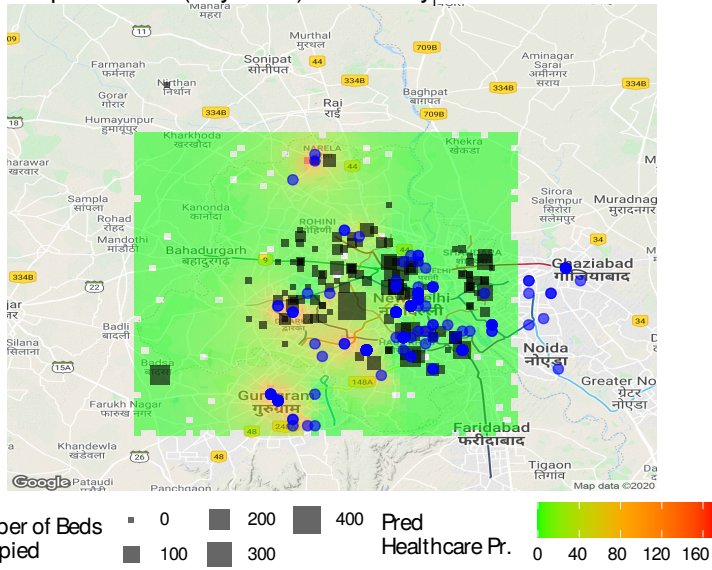
Arbab Goswami has resigned from Editor's Guild, which has no credibility left, and its bias is not even subtle. Not even a word on #PaighatLynching by the Guild. They have been silent on fake news stories during COVID. Courage to speak truth is absent. #ArbabGoswami

Click a point on the chart to see the most popular tweet

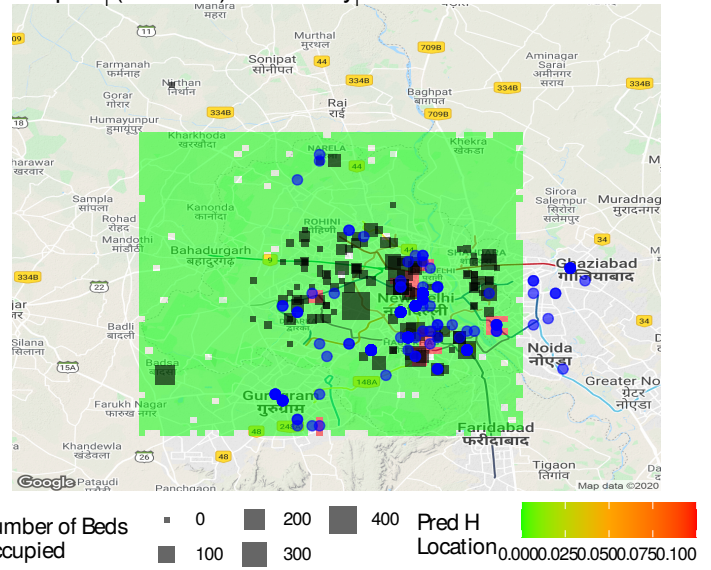
Figure 6:

Figure 7:

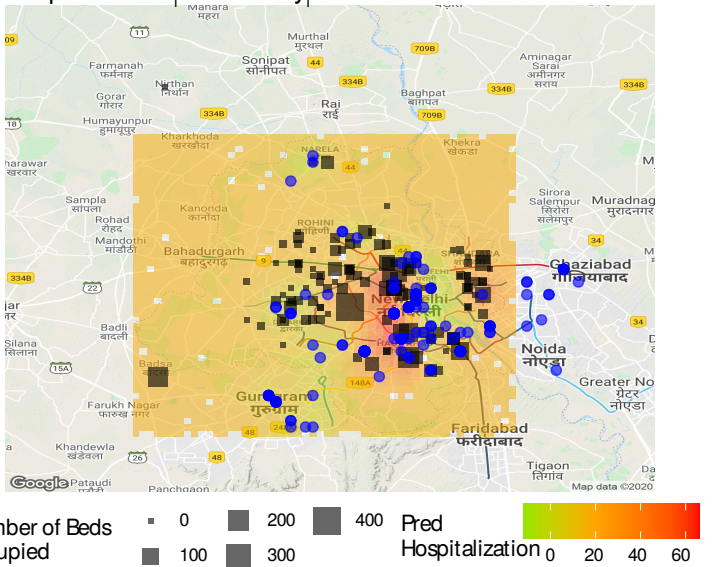
A Hospitalization (City Scale) ~ Positivity



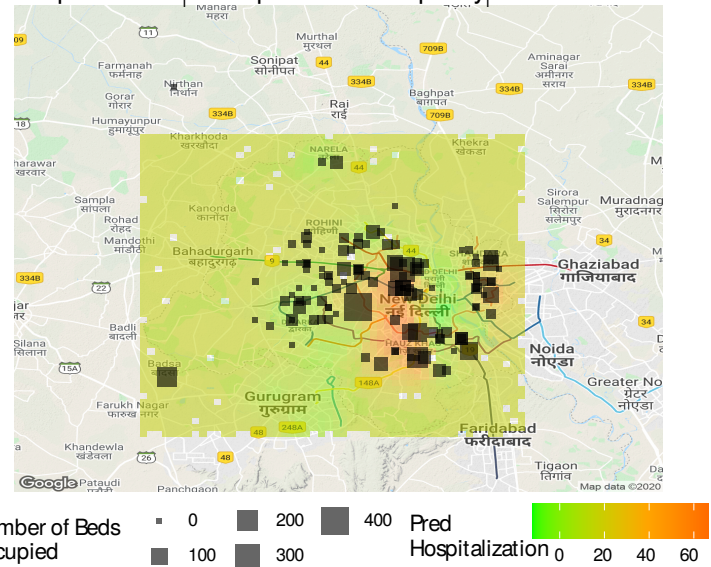
B Hospital (Location) ~ Positivity



C Hospitalization_i ~ Positivity_i



D Hospitalization_i ~ Hospital Bed Occupancy



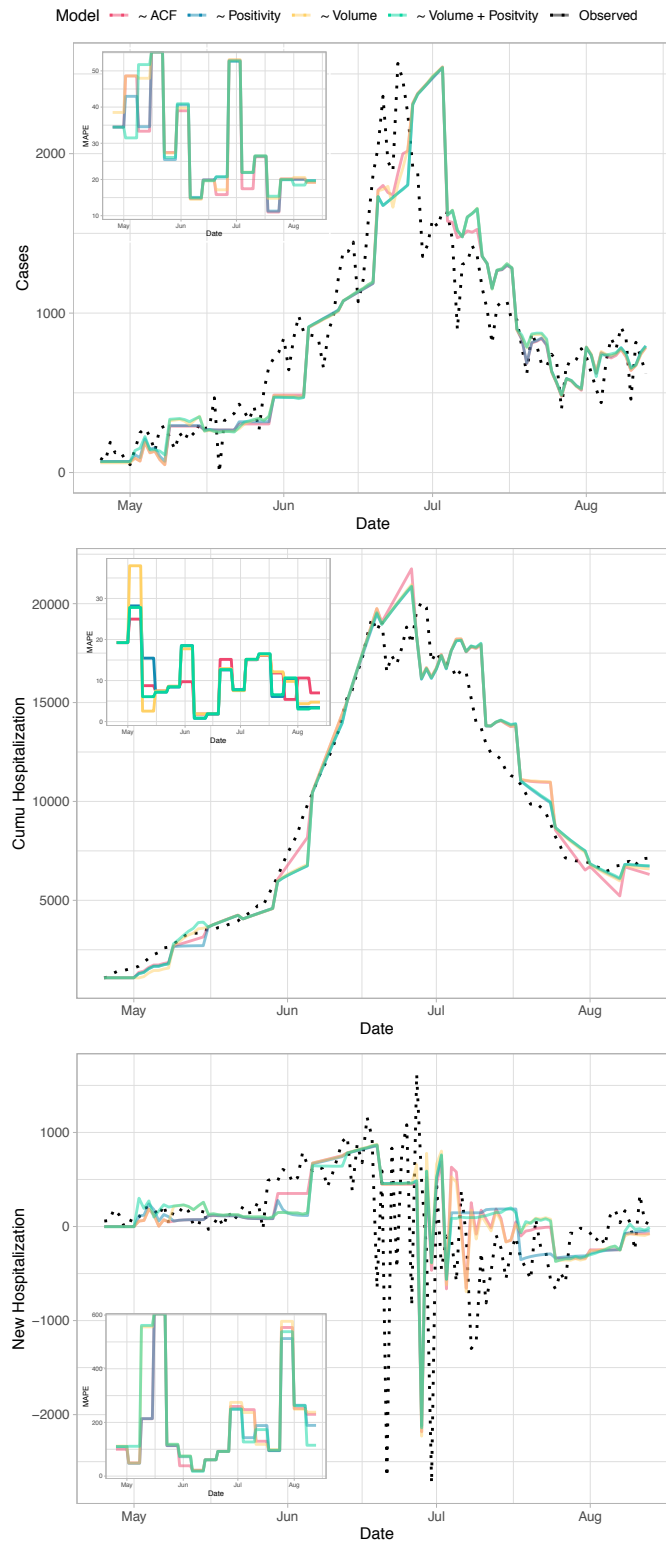


Figure 8: